

Specificity-aware reinforcement learning for fine-grained open-world classification

Samuele Angheben^{1,2} Davide Berasi¹ Alessandro Conti¹ Elisa Ricci^{1,2} Yiming Wang²

¹University of Trento ²Fondazione Bruno Kessler

Abstract

Classifying fine-grained visual concepts under open-world settings, i.e., without a predefined label set, demands models to be both accurate and specific. Recent reasoning Large Multimodal Models (LMMs) exhibit strong visual understanding capability but tend to produce overly generic predictions when performing fine-grained image classification. Our preliminary analysis reveals that models do possess the intrinsic fine-grained domain knowledge. However, promoting more specific predictions (specificity) without compromising correct ones (correctness) remains a non-trivial and understudied challenge. In this work, we investigate how to steer reasoning LMMs toward predictions that are both correct and specific. We propose a novel specificity-aware reinforcement learning framework, *SpeciaRL*, to fine-tune reasoning LMMs on fine-grained image classification under the open-world setting. *SpeciaRL* introduces a dynamic, verifier-based reward signal anchored to the best predictions within online rollouts, promoting specificity while respecting the model’s capabilities to prevent incorrect predictions. Our out-of-domain experiments show that *SpeciaRL* delivers the best trade-off between correctness and specificity across extensive fine-grained benchmarks, surpassing existing methods and advancing open-world fine-grained image classification. Code and model are publicly available at <https://github.com/s-angheben/SpeciaRL>.

1. Introduction

Image classification has long been a cornerstone problem in computer vision, aiming to assign a semantic concept to the main object featured in an image [12]. Traditional image classification models typically operate under a *closed-world* setting, where all possible semantic categories are predefined within a fixed vocabulary [40]. However, in real-world environments models often need to handle emerging categories or novel concepts, highlighting the importance of *open-world* classification [5], which removes the fixed vocabulary assumption. This more challenging and practically relevant setting can now be studied more effectively thanks to the emergence of large pre-trained vision–language models [39, 60]. Candidate concepts can be derived from large

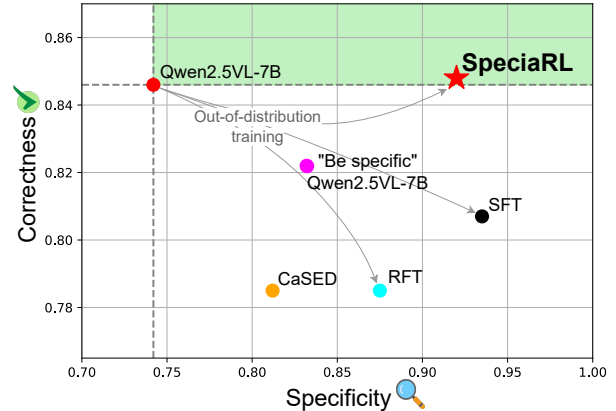


Figure 1. In open-world image classification, improving prediction specificity without compromising correctness remains challenging. Existing techniques, such as prompting to be specific, supervised fine-tuning (*sft*) or reinforcement fine-tuning (*rft*), promote specificity but reduce correctness. Instead, our proposed method (**SpeciaRL**) significantly improves the specificity of the base Qwen2.5VL-7B model without compromising correctness. Gray arrows indicate that training is performed on a single-domain (bird) dataset, which is disjoint from the domains in the test set, therefore illustrating cross-domain generalization.

textual corpora [9] or directly generated by recent Large Multimodal Models (LMMs) [4, 8, 26, 28, 65] in response to open-ended prompts such as “*What is the object in the image?*”. Such advances have, in turn, motivated novel approaches as well as new evaluation protocols to assess the correctness of predicted concepts, addressing the unconstrained nature of LMM-generated outputs.

Recent benchmarking works [10, 31, 63] extensively evaluated the classification performance of LMMs in both closed-world and open-world settings. Focusing on the latter, Conti *et al.* [10] introduced performance metrics based on large language models and textual embedding similarity, in an effort to comprehensively describe the behavior of LMMs. The study showed that the best-performing models are recent *reasoning LMMs*, such as Qwen2.5VL [3], which are trained with reasoning-enriched multimodal datasets to connect visual evidence with linguistic inference. The study also revealed that *LMMs mostly struggle in classifying fine-*

Corresponding author: sangheben@fbk.eu.

grained concepts, with the *tendency of being overly generic* (e.g., flower vs. daisy). However, naïvely encouraging more specific predictions (i.e., high specificity) may increase the number of wrong outputs (i.e., reduced correctness). For example, Conti *et al.* observed in [10] that simple prompting benefits LMMs in producing more fine-grained predictions, but at the cost of inferior correctness. Our own experimentation also confirms this compromised correctness when promoting specificity, either by directly querying the model to “be specific” or by fine-tuning the model with supervised fine-tuning (*sft*) or reinforcement fine-tuning (*rft*), as shown in Fig. 1. Promoting more specific predictions requires indeed a delicate *balance between specificity and correctness*, a non-trivial challenge that remains greatly underexplored.

This work addresses the limitation of LMMs being overly generic on fine-grained open-world classification, aiming to improve prediction *specificity* without compromising *correctness*. Before designing the method, we conduct an in-depth inspection of the models’ behavior to understand their capabilities and limitations. We analyzed the prediction distribution over several specificity levels, e.g., *more specific*, *specific*, *less specific*, and *generic*, confirming the tendency of the model being overly generic. We further verify whether this limitation stems from a lack of domain-specific knowledge. Interestingly, our preliminary analysis on Qwen2.5VL [3], the best-performing LMM in [10], suggests that *the model does possess substantial prior knowledge*, as evidenced by its strong ability to correctly identify fine-grained categories when queried multiple times, despite a few samples remaining generic or less specific.

Given these observations, we propose SpeciaRL, an effective reinforcement learning method with a novel specificity-aware dynamic reward design to elicit specificity within the model’s maximal capabilities. Intuitively, if a model’s best prediction for a given sample is inherently generic, penalizing it for lacking specificity may push it toward producing more incorrect outputs. Our *sample-wise* reward is therefore *dynamically* set based on the highest specificity level the LMM can achieve for that sample during multiple rollouts. This paradigm naturally blends into the GRPO [41] algorithm without compromising computational efficiency. SpeciaRL encourages the model’s genuine reasoning capability in fine-grained visual understanding, enabling *strong out-of-domain generalization* even when trained on a limited dataset from a specific domain. Empirically, SpeciaRL strikes the best balance between specificity and correctness across both *fine-grained* and *very fine-grained* datasets, outperforming zero-shot reasoning LMMs and fine-tuned baselines.

Our main **contributions** are summarized below:

- We tackle the non-trivial, underexplored challenge of promoting specificity without compromising correctness in fine-grained open-world image classification.
- Our analysis confirms that LMMs are overly generic and

provides insights on their potential and limitation.

- We introduce SpeciaRL, an online reinforcement learning method with a novel specificity-aware dynamic reward.
- SpeciaRL achieves the best trade-off between specificity and correctness compared to existing methods.

2. Related Works

Large Multimodal Models and reasoning. Early vision-language models primarily focused on learning a joint embedding space that aligned textual and visual representations [19, 39, 60]. This paradigm later evolved into *generative* Large Multimodal Models [2, 8, 27, 28, 43, 52, 65], which connect visual features from a pretrained encoder to the input space of a Large Language Model, enabling open-ended visual question answering and visual reasoning.

Recent studies on Chain-of-Thought (CoT) prompting [20, 53] have demonstrated that eliciting multi-step reasoning in LMMs significantly improves their performance on several tasks. This insight has led to the development of *reasoning* LMMs such as OpenAI o1 [18] and DeepSeek-R1 [16], which are specifically fine-tuned to perform complex multi-step reasoning before providing a final answer. In this context, Reinforcement Learning has emerged as an efficient and effective post-training strategy for improving the reasoning capabilities of LMMs [1, 37, 45, 66].

In this paper, we aim to investigate and improve the capabilities of reasoning LMMs in the specific task of open-world image classification, promoting specificity without compromising correctness.

Evaluating LMMs as image classifiers. Evaluating the performance of LMMs is challenging due to their unconstrained output space. Several comprehensive benchmarks have been introduced to test the general capabilities of LMMs [14, 25, 29, 32, 64]. However, the specific problem of evaluating LMMs as image classifiers, that is, assessing their ability to assign a semantic concept to a visual input, has received less attention [10, 31, 57, 63]. Existing approaches reformulate classification as a multiple-choice visual question answering task [48], or estimate accuracy based on next-token prediction probabilities [57]. Most relevant works include the study [44] on the quantification of prediction quality with hierarchical precision and recall, mapping open-ended predictions onto a predefined taxonomy through a combination of string matching and semantic similarity measures, and the benchmark [10] featuring an extensive evaluation of how various LMMs respond to the question “What is the main object in the image?”, introducing four complementary metrics to assess different aspects of open-world prediction behavior.

Instead, we leverage the judgment of a LLM-based verifier to automatically assess and categorize the relationships between the predictions and ground-truth labels.

Reinforcement Learning. Reinforcement Learning [47]

is currently the main post-training paradigm for improving the reasoning capabilities of LLMs and LMMs. Early work on RL from Human Feedback (RLHF) [37, 45] leveraged human preference annotations as reward signals, guiding models toward being more helpful, harmless, and aligned with human preference. More recently, RL with Verifiable Rewards (RLVR) has emerged as an effective strategy for improving reasoning [16, 23, 49]. Instead of relying on subjective human feedback, RLVR utilizes rule-based or programmatically verifiable reward signals obtained by directly checking model outputs against ground-truth targets. This makes RLVR particularly suitable for tasks with structured solutions, such as mathematical problem solving [41, 54, 55] and code generation [17, 61]. Notably, the Group Relative Policy Optimization (GRPO) [41] algorithm, popularized by DeepSeek-R1 [16], has shown exceptional performance. GRPO has been successfully applied also in vision tasks [30, 34]. Closely related to our work, Visual-RFT [34] applies verifiable rewards to closed-set image classification, rewarding predictions that exactly match target labels.

Given the verifiable reward assumption, RLVR has been mainly employed on tasks with structured solutions. However, recent works [15, 46] have overcome this limitation and extended the RLVR paradigms to other domains with the help of a model-based verifier for the reward computation.

In this work, we build upon these ideas and propose a novel RL framework for open-world image classification, compatible with on-policy optimization methods such as GRPO. Our method leverages an LLM-based verifier to provide reward signals to open-ended predictions within the huge unconstrained LMMs output space.

3. Method

In this section, we first revisit the task of open-world image classification [10], outlining our primary objective (Sec. 3.1). Then, we introduce how to assess model predictions to quantify their specificity and correctness (Sec. 3.2). Next, we conduct a preliminary analysis to further inspect the prediction behavior of the best-performing reasoning LMM, examining its capabilities and limitations in classifying fine-grained concepts under the open-world setting (Sec. 3.3). Finally, motivated by our preliminary findings, we introduce SpeciaRL, an online RL fine-tuning approach with a novel dynamic reward design that encourages more specific predictions without increasing incorrect ones (Sec. 3.4).

3.1. Problem formulation

We consider the problem of classifying an image in an open-world setting, where the set of possible output classes is neither predefined nor finite. Formally, we aim to learn a classifier $f : \mathcal{V} \rightarrow \mathcal{S}$, which maps an image $I \in \mathcal{V}$ to a semantic concept $s \in \mathcal{S}$. Here, \mathcal{S} denotes a huge semantic space including all the concepts that can be expressed in

natural language through concise labels. In our setting, f corresponds to a Large Multimodal Model Φ_{LMM}^θ with learnable parameters θ , and \mathcal{S} includes all the concepts that can be expressed with the model’s vocabulary.

Semantic concepts within \mathcal{S} are not independent but semantically related following complex and hierarchical ontologies [44]. For instance, a *golden-winged warbler* is a type of *warbler* and more broadly a *bird*. The unconstrained nature of the open-world setting, and the generative nature of Φ_{LMM}^θ , can produce multiple possible labels that are *correct at different levels of specificity*. As revealed in [10], existing LMMs tend to produce **correct but generic** predictions, particularly in fine-grained domains. As shown in [10], while eliciting LMMs to be more specific through the input prompt can benefit models in producing more specific predictions, this also comes at the cost of correctness, resulting in more wrong predictions. How to balance the specificity and correctness remains a non-trivial challenge [44].

This work focuses on addressing the limitation of LMMs being overly generic in open-world image classification. We aim to promote both *specificity and correctness*, *i.e.*, generating correct predictions with maximal specificity without harming their correctness.

3.2. Prediction Evaluation

Before method development, we first need to assess both the *correctness* and the *specificity* of model predictions. Previous work on hierarchical classification [44] relies on explicit taxonomies to measure the semantic distance between labels. However, given the open nature of our setting, we do not assume a predefined hierarchy, which is also challenging to acquire. The recent benchmark [10] introduces metrics to measure semantic similarity via both LLMs and pre-trained encoders, from which the authors broadly categorize the predictions into specific *vs.* generic, and correct *vs.* incorrect. Our extensive qualitative analysis reveals that the possible relations between a prediction p and the fine-grained ground-truth label y are much richer: the prediction can be generic or less specific than its ground-truth label, and the model may also abstain when it judges a lack of knowledge. However, it is not easy to manipulate these soft metrics, which are introduced to reflect the rich possibilities of model predictions. In this work, we leverage a strong LLM as the judge categorizing the relations between the prediction p and its fine-grained ground-truth label y .

Prediction categorization. We identify a set $\mathcal{C} = \{W, A, G, S^-, S, S^+\}$ of six mutually exclusive categories that comprehensively cover the main possible relations:

- **Wrong** (W): the prediction is incorrect, referring to a different concept from the target.
- **Abstain** (A): the prediction is a refusal to answer, which we deem as the least informative non-Wrong response a model could provide.

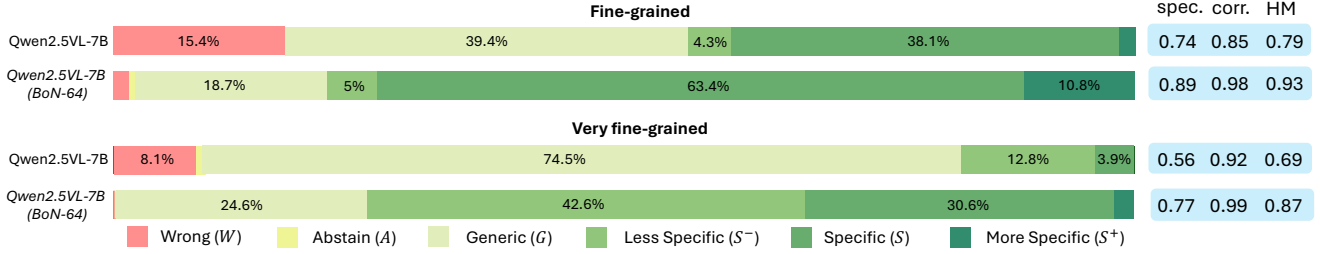


Figure 2. Predictions distribution over categories for Qwen2.5VL-7B [3] and its BoN version with $N = 64$ inference runs. The right side shows specificity, correctness and their harmonic mean (HM). The BoN-64 serves as an indication for the model’s potential capability.

- **Generic (G)**: the prediction is correct, but represents a significantly broader category than the ground-truth. For example, $p = \text{dog}$, $y = \text{samoyed}$.
- **Less Specific (S^-)**: the prediction is correct but corresponds to a closely related parent category of the ground-truth. For example, $p = \text{warbler}$, $y = \text{golden-winged warbler}$.
- **Specific (S)**: the prediction is an exact match or a direct synonym for the ground-truth.
- **More Specific (S^+)**: the prediction refers to a more specific subtype or instance of the ground-truth. This is unlikely given that the target is a fine-grained concept, but it may occur in practice.

Note that these categories are naturally ordered from the least to the most informative as:

$$W \prec A \prec G \prec S^- \prec S \prec S^+ \quad (1)$$

So, given two predictions p, p' respectively categorized as c, c' , our objective considers p to be better than p' if $c \succ c'$.

To automatically categorize predictions, we adopt an LLM-as-a-judge approach. We prompt a Large Language Model Ψ_{LLM} to provide a suitable category $c_y(p) \in \mathcal{C}$ for a given prediction p and ground-truth label y :

$$c_y(p) = \Psi_{\text{LLM}}(\langle p, y \rangle, P_j), \quad (2)$$

Here, the judge’s prompt P_j defines each category with precise descriptions. To ensure a wide range of prior knowledge and reliable evaluation of fine-grained semantics, we employ Llama3-72B [13] as the judge. The exact expression of P_j is detailed in *Supp. Mat.*

Specificity and Correctness measures. We quantify the *specificity* and *correctness* based on the above-described categorization. Considering a dataset $\mathcal{D} = \{(I_i, y_i)\}_{i=1}^n$ of n labeled images, we indicate with c_i the category of prediction $\Phi_{\text{LLM}}^\theta(I_i, P_c)$ and with $n_W = \#\{i \mid c_i = W\}_{i=1}^n$ the number of Wrong (W) predictions. We define *correctness* as the percentage of non-Wrong predictions:

$$\text{correctness} = 1 - \frac{n_W}{n}. \quad (3)$$

To measure the specificity, we assign a specificity score $s(c)$ to each non-Wrong category as follows:

$$s(A) = 1, s(G) = 2, s(S^-) = 3, s(S) = s(S^+) = 4. \quad (4)$$

Intuitively, consider the path over the categories from the root A to the leaf S^+ . The score in Eq. (4) is the length of the intersection between the path from the root to the prediction’s category c and the path from the root to the ground-truth category S . In other words, this can be seen as the amount of information provided by the prediction about the ground-truth concept. We then define *specificity* as the average normalized score over the non-Wrong predictions:

$$\text{specificity} = \frac{1}{n - n_W} \sum_{c_i \neq W} \frac{s(c_i)}{4}. \quad (5)$$

Note that specificity lies in $[0, 1]$ and it is 0.5 if all the correct predictions are Generic. Finally, we consider the harmonic mean (HM) as a quantitative measure of overall performance:

$$\text{HM} = 2 \frac{\text{specificity} \times \text{correctness}}{\text{specificity} + \text{correctness}}. \quad (6)$$

3.3. On LMMs being overly generic

We conduct a preliminary study to gain a detailed understanding of the models’ prediction behaviors in terms of correctness and specificity, aiming to identify their capabilities and limitations. We base our analysis on recent reasoning LMMs as they demonstrate the best performance on open-world image classification [10].

Experiment setting. We use the *fine-grained* set from [10], consisting of fine-grained image classification benchmarks where classes belong to a shared superclass and/or are challenging to distinguish. This includes Flowers102 [36] (flowers), Food101 [6] (food), and OxfordPets [38] (animals). We also consider the *very fine-grained* set, where categories are not only within the same subclass but also highly difficult to differentiate. This includes StanfordCars [21], where labels specify car brands, models, and years of production, and FGVCAircraft [35], which categorizes aircraft models.

Each image I in a dataset is associated with a human-annotated ground-truth label $y \in \mathcal{S}$. The model’s prediction $p \in \mathcal{S}$ is obtained by prompting the reasoning LMM Φ_{LMM}^θ :

$$p = \Phi_{\text{LMM}}^\theta(I, P_c) \quad (7)$$

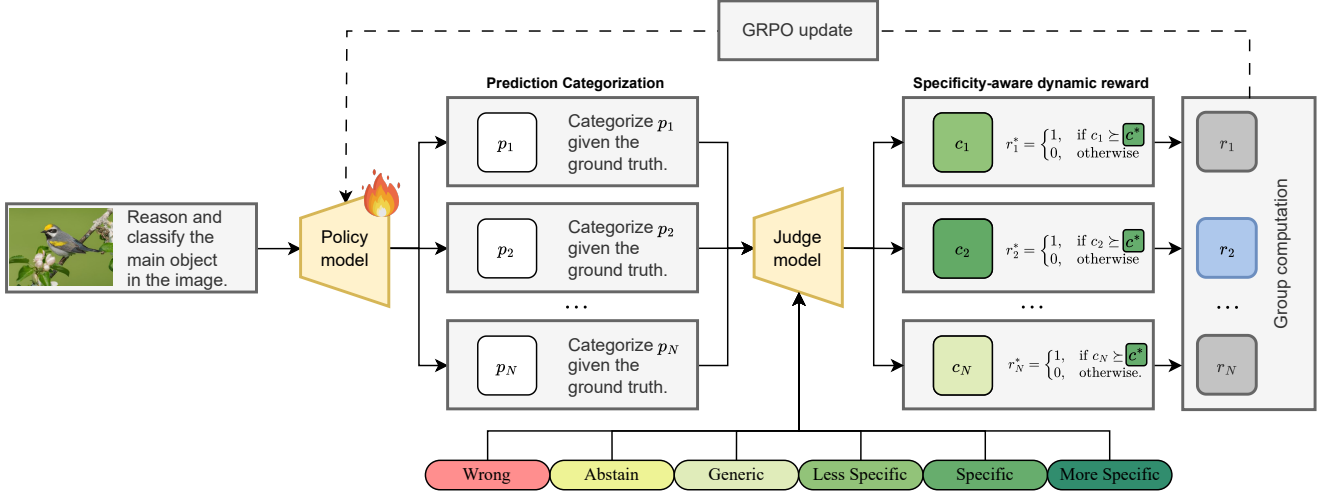


Figure 3. Overview of **SpeciaRL**. Given an input image I , the policy model generates N open-ended predictions $\{p_1, \dots, p_N\}$. Each prediction is categorized by a judge model (LLM verifier) as wrong or correct at different levels of specificity with respect to the ground-truth. A verifiable reward r_i^* is then assigned according to whether the prediction’s category c_i meets the adaptive reference level c^* , which is defined based on the best prediction within the N rollouts. The resulting graded rewards are aggregated through a Group Relative Policy Optimization (GRPO) update to reinforce policies that are maximally specific while remaining correct.

where P_c is a text prompt querying the model to classify the main object in the images by first reason on the input and then including the final prediction in `<answer>` tags. We report the exact expression of our prompt in the *Supp. Mat.*. Specifically, we consider Qwen2.5VL-7B [3] as Φ_{LLM}^θ , which can perform visual understanding with linguistic reasoning and follow the thought-answer template for the output.

How specific are model predictions? Figure 2 (Row I&III) shows the percentage of predictions within each category, as well as their correctness and specificity scores. The model predictions are mostly correct, but with a clear tendency towards being generic, as already observed in [10]. This inclination is more evident in the case of the very fine-grained set (Row III), where almost 75% of the predictions are Generic.

Does the model have prior domain knowledge? We wonder whether the tendency to be generic is due to the lack of domain-specific knowledge. We evaluate this aspect by considering the best prediction over N rollouts based on the intuition that the model may possess the prior knowledge to produce better predictions, but it may be inefficient in sampling the correct reasoning path in a single attempt [58]. Specifically, we define the Best-of-N (BoN) prediction for a given sample (I, y) as the prediction within N generations $\{p_1, \dots, p_N\}$ with the most informative category:

$$\text{BoN}_y(I) = \arg \max_{p \in \{p_1, \dots, p_N\}} \Psi_{\text{LLM}}(\langle p, y \rangle, P_j). \quad (8)$$

We set $N = 64$, a computationally reasonable value that is sufficiently large to provide a reliable upper bound on the model classification capability.

As shown in Fig. 2 (Row II&IV), the best prediction within 64 rollouts (BoN-64) shows significantly *greater*

specificity and correctness compared to one-time inference, as evident in both the distribution over categories and the metric scores. This suggests that the model *does possess the prior knowledge* to be substantially more precise, despite its generic tendency. We hypothesize that this might be due to the bias inherited from the pretraining distribution, where generic concepts are much more frequent than specific ones. On the other hand, the BoN-64 results reveal that, even at its best, the LMM still produces a decent portion of Generic or Less Specific predictions, particularly in very fine-grained cases. This suggests some samples still lie outside the model’s capabilities. These findings raise a compelling question: Is it possible to steer the model towards more specific predictions, approaching the BoN-64 performance, without pushing it over its actual potential, to avoid increasing incorrect answers?

3.4. Specificity-aware Reinforcement Learning

In our preliminary analysis, we observed that pretrained LMMs lack specificity in their classification predictions, tending toward generic responses. Importantly, we noted this is not due to a lack of prior knowledge. For this reason, we propose a fine-tuning strategy that guides the model’s behavior to optimize its capability to provide correct and specific predictions. Given that the base model possesses a good level of prior knowledge, we do not aim to inject new knowledge into the model, but rather, we seek to improve its sampling efficiency and reasoning capabilities. For this reason, we adopt a reinforcement learning approach, which is highly effective in steering the model’s behavior and increasing reasoning performance [16, 23, 49]. Specifically,

we leverage the previously defined LLM-as-a-judge categorization to construct an outcome reward feedback to guide this optimization during training.

Reinforcement Learning with Verifiable Rewards enables fine-tuning a model using a simple rule-based reward signal on tasks where a prediction is directly verifiable against the correct answer. Originally proposed to improve LLMs’ performance on language tasks such as math and coding [16], RLVR has recently been shown to be effective in vision tasks as well [30, 34]. Among RLVR algorithms, we adopt GRPO [41] for its efficiency and effectiveness. At its core, GRPO generates groups of diverse outputs $\{p_1, \dots, p_N\}$ and optimizes to incentivize responses with higher rewards within each group. The core of RLVR is the definition of the reward signal. Given label y and a model prediction $p = \Phi_{\text{LLM}}^\theta(I, P_c)$, a standard verifiable reward is defined as:

$$r(p, y) = \begin{cases} 1, & \text{if } p = y, \\ 0, & \text{otherwise.} \end{cases} \quad (9)$$

Note that this simple definition assumes the possibility of directly comparing a prediction against the target solution.

Specificity-aware dynamic reward. Considering that, in an open-world setting, a prediction can be correct at different specificity levels, the standard reward could risk pushing the model to be *overly specific at the cost of correctness*. We therefore design a custom reward signal suited for open-world classification. For a given sample (I, y) , we argue that any correct prediction, even if it does not match the ground-truth label, should be positively rewarded if it achieves the model’s maximum potential. Formally, we use the best prediction category within N runs $c_{\text{best}} = c_y(\text{BoN}_y(I))$ to define a minimal specificity requirement $c^* \in \mathcal{C}$ to be positively rewarded, accounting for the corner cases $c_{\text{best}} \in \{S^+, W\}$:

$$c^* = \begin{cases} S, & \text{if } c_{\text{best}} = S^+ \\ A, & \text{if } c_{\text{best}} = W \\ c_{\text{best}}, & \text{otherwise.} \end{cases} \quad (10)$$

Our sample-specific reward for a prediction p is defined as:

$$r_I^*(p, y) = \begin{cases} 1, & \text{if } c_y(p) \succeq c^* \\ 0, & \text{otherwise.} \end{cases} \quad (11)$$

This reward is therefore positive when the prediction is Specific, More Specific, or at least as informative as the best prediction within the current model’s capability. For example, a Generic prediction receives a positive reward if the BoN prediction is also Generic, but it is not rewarded if the BoN is Specific or Less Specific. Wrong predictions always receive reward 0.

We compute the BoN prediction in an *online* manner, that is, with the current weights of the model. Specifically, we

use the N rollouts of the GRPO algorithm. This makes the reward computation efficient, as it does not require any additional generations compared to the static reward in Eq. (9).

4. Experiments

In this section, we first describe the experimental setup, specifying the datasets, evaluation protocols and training details. Then, we present comparative analysis against state-of-the-art methods, supported by qualitative examples, proving SpeciaRL achieves the best specificity-correctness trade-off (Sec. 4.1). Finally, we show ablation studies on our key design choices on the dynamic reward (Sec. 4.2).

Datasets. For the evaluation, we use the same *fine-grained* and *very fine-grained* datasets as detailed in Sec. 3.3. For training, we randomly select 3000 samples from the CUB dataset [51], a bird species classification dataset with *fine-grained* annotations. Note that training and testing data are from different domains. All evaluations are therefore conducted in an *out-of-domain* setting to assess generalization and reasoning capabilities rather than memorization.

Evaluation metrics. Model predictions are obtained using the same prompting strategy described in Sec. 3.3. We evaluate both *specificity* and *correctness*, as well as their harmonic mean (HM) defined in Sec. 3.2. The HM captures how well a model balances specificity and correctness, providing a single scalar measure of overall performance. For completeness, we also report the proportion of predictions assigned to each category by the LLM judge. To position our SpeciaRL in the literature, we also follow the general-purpose evaluation protocol introduced in [10], assessing performance using LLM evaluation, string matching and semantic similarity between model’s outputs and ground-truth labels. While useful for indicating overall performance, these metrics are not specifically designed to quantify specificity and correctness.

Training details. We use Qwen2.5VL-7B as the base model. Training is performed with Group Relative Policy Optimization with the following configuration: number of rollouts per sample: $N = 10$, training batch size: 256, learning rate: $\eta = 3 \times 10^{-5}$, total training epochs: 15, and KL penalty coefficient: $\lambda = 0.01$. For reward computation, we use Qwen3-30B-A3B-Instruct-2507-FP8 [50] as the external LLM judge. Note that this is different from the Llama3-72B [13] model used for evaluation. This distinction avoids the influence of family-specific biases and ensures a fair evaluation. All reinforcement learning experiments are implemented using the Verl framework [42].

4.1. Main comparison

Baselines. We compare SpeciaRL against both zero-shot and training-based baselines. For zero-shot methods, we consider both the retrieval-based CaSED [9], which exploits CLIP [39] to retrieve candidate concepts from web-scale textual corpus, and state-of-the-art reasoning LMMs, including

Table 1. Open-world image classification results of **zero-shot** methods and models **fine-tuned out-of-domain**. We report the ratio of the predictions within categories assigned by the LLM verifier, our measures of specificity and correctness and the harmonic mean of these two (HM). Results are averaged over all datasets within the **fine-grained** and **very fine-grained** sets. For reference, we report the performance of inference out of 64 runs (BoN-64). Best in **bold**; second best underlined.

Model	Fine-grained							Very fine-grained										
	Prediction categorization						Metrics			Prediction categorization						Metrics		
	S^+	S	S^-	G	A	W	spec. \uparrow	corr. \uparrow	HM \uparrow	S^+	S	S^-	G	A	W	spec. \uparrow	corr. \uparrow	HM \uparrow
CaSED [9]	0.0%	43.7%	10.6%	24.2%	0.0%	21.5%	0.812	0.785	0.797	0.0%	0.9%	13.8%	56.0%	0.0%	29.3%	0.56	0.707	0.612
InternVL2.5-4B [7]	0.0%	11.4%	1.5%	54.4%	8.4%	24.1%	0.554	0.759	0.639	0.0%	0.1%	1.2%	62.7%	5.5%	30.5%	0.486	0.695	0.571
InternVL2.5-8B [7]	0.7%	16.7%	3.3%	30.6%	20.7%	27.9%	0.575	0.721	0.624	0.0%	1.2%	5.7%	54.5%	15.6%	22.9%	0.476	0.771	0.589
Qwen2.5VL-3B [4]	0.8%	17.3%	2.7%	53.4%	4.2%	21.5%	0.608	0.785	0.685	0.1%	1.1%	3.9%	75.1%	2.4%	17.4%	0.511	0.826	0.631
Qwen2.5VL-7B [4]	1.4%	38.1%	4.3%	39.4%	1.4%	15.4%	0.742	<u>0.846</u>	0.790	0.1%	3.9%	12.8%	74.5%	0.6%	8.1%	0.555	0.919	0.692
Qwen2.5VL-7B (“Be specific”)	2.1%	49.1%	6.2%	22.4%	3.4%	16.8%	0.816	0.832	0.822	0.3%	12.5%	29.3%	45.6%	1.3%	11.0%	0.652	<u>0.89</u>	0.751
Qwen2.5VL-7B (<i>sft</i>)	2.4%	64.4%	7.6%	6.0%	0.3%	19.3%	0.935	0.807	<u>0.866</u>	0.5%	22.5%	50.8%	11.8%	0.1%	14.3%	0.789	0.857	0.814
Qwen2.5VL-7B (<i>rft</i>)	4.6%	52.2%	5.0%	16.2%	0.0%	21.5%	0.875	0.785	0.825	1.2%	24.7%	53.9%	3.5%	0.0%	16.7%	0.825	0.833	<u>0.821</u>
SpeciaRL-7B	5.6%	63.4%	5.1%	10.7%	0.0%	15.2%	<u>0.920</u>	0.848	0.883	1.0%	25.2%	54.2%	5.1%	0.0%	14.5%	<u>0.818</u>	0.855	0.830
Qwen2.5VL-7B (BoN-64)	10.8%	63.4%	5.0%	18.7%	0.6%	1.6%	0.889	0.984	0.933	1.9%	30.6%	42.6%	24.6%	0.1%	0.2%	0.77	0.998	0.868

Qwen2.5VL-(3B & 7B) [3] and InternVL2.5-(4B & 8B) [8], to examine performance across architectures and scales. We also elicit Qwen2.5VL-7B to be specific in its predictions via prompting (“Be specific”).

For training-based methods, we consider fine-tuning the strongest reasoning LMM Qwen2.5VL-7B, with supervised fine-tuning (*sft*) and reinforcement fine-tuning (*rft*). Specifically, Qwen2.5VL-7B (*sft*) performs supervised fine-tuning by cross-entropy loss on a custom dataset of high-quality reasoning traces constructed similarly to [59, 62]. Precisely, for each training sample, we prompt the base model to generate a reasoning-answer pair leading to the correct ground-truth label. We opt to use the same base model to avoid introducing extra knowledge into the model. Qwen2.5VL-7B(*rft*) is trained with GRPO using the common static reward signal, which assigns positive feedback only to predictions matching the ground-truth. In our setting, this corresponds to a reward 1 when the prediction is categorized as Specific (S) or More Specific (S^+), 0 otherwise.

Finally, we report the Best-of-64 performance defined in Sec. 3.3 as an empirical upper bound on the base model’s potential capabilities.

Quantitative results. As shown in Tab. 1, the retrieval-based method CaSED [9] achieves promising specificity, while all zero-shot reasoning LMMs are limited in specificity as they produce mostly Generic predictions. Eliciting specificity through the prompt, *i.e.* Qwen2.5VL-7B(“Be specific”), reduces Generic predictions, but also leads to more Wrong predictions. On the other hand, all training-based approaches substantially improve specificity. Yet, on balancing specificity and correctness, SpeciaRL achieves the best performance with the highest HM across both test groups, with less compromise on correctness. Notably, on the **fine-grained** dataset, SpeciaRL improves both specificity and correctness compared to the base Qwen2.5VL-7B model. Please refer to *Supp. Mat.* for the performance on each

Table 2. Comparison against state-of-the-art methods following the evaluation protocol of [10]. Key: TI:Text Inclusion; LI: Language Inclusion; SS: Semantic Similarity; CS: Concept Similarity. Best in **bold**; second best underlined.

Model	Fine-grained				Very fine-grained			
	TI \uparrow	LI \uparrow	SS \uparrow	CS \uparrow	TI \uparrow	LI \uparrow	SS \uparrow	CS \uparrow
<i>Retrieval-based baselines</i>								
CASED	27.4	46.6	60.7	61.7	0.7	47.1	38.5	38.5
CLIP retrieval	32.4	45.4	42.9	65.4	7.0	18.1	39.7	56.1
<i>Non-reasoning LMMs</i>								
IDEFICS2 8B	3.0	49.9	38.0	41.7	0.0	67.0	29.6	33.6
INSTRUCTBLIP Vic 7B	10.4	48.8	35.6	47.2	0.0	61.0	30.0	34.3
INTERNVL2 2B	14.9	47.0	31.6	50.7	0.7	32.9	33.1	43.9
INTERNVL2 4B	16.2	44.4	32.0	52.0	1.7	36.8	33.8	44.2
INTERNVL2 8B	22.3	46.7	34.8	56.7	2.3	32.5	36.0	49.4
LLAVA-1.5 7B	8.4	46.5	28.2	44.8	0.0	41.0	28.6	37.6
LLAVA-NEXT Mist 7B	26.8	43.7	35.3	60.1	1.4	47.2	34.2	46.9
LLAVA-NEXT Vic 7B	16.9	44.5	32.2	53.2	1.3	42.2	34.5	46.1
LLAVA-OV Qwen2 0.5B	6.0	42.7	38.5	43.3	0.6	65.6	30.5	37.1
LLAVA-OV Qwen2 7B	6.4	40.4	39.0	43.8	0.0	76.7	31.9	32.4
PHI-3-VISION	13.4	49.1	31.8	47.2	0.2	45.0	28.9	36.0
QWEN2VL 2B	35.7	62.5	40.7	63.4	12.9	60.7	45.1	62.3
QWEN2VL 7B	34.6	64.0	39.2	62.9	0.8	63.0	34.5	43.4
<i>Reasoning LMMs</i>								
INTERNVL2.5 2B	12.2	38.6	27.5	47.0	0.8	52.4	31.6	41.5
INTERNVL2.5 4B	17.2	48.2	32.8	52.3	0.5	55.6	31.4	39.7
INTERNVL2.5 8B	17.9	50.9	32.8	53.5	1.6	59.9	32.1	40.4
QWEN2.5VL 3B	44.3	63.9	41.6	69.3	9.4	58.9	39.9	58.5
QWEN2.5VL 7B	58.7	74.2	47.0	78.9	16.4	70.4	45.8	68.4
<i>Reasoning LMMs - fine-tuned out-of-distribution</i>								
Qwen2.5VL-7B (<i>sft</i>)	60.0	73.8	47.8	80.1	17.1	71.1	47.3	71.1
Qwen2.5VL-7B (<i>rft</i>)	<u>62.0</u>	74.8	<u>48.4</u>	<u>80.6</u>	<u>21.9</u>	<u>68.2</u>	<u>49.5</u>	<u>74.0</u>
SpeciaRL-7B	62.7	<u>74.4</u>	49.2	81.1	24.9	63.8	50.5	75.4

individual test dataset and additional prompting baselines.

Moreover, Tab. 2 reports the performance of SpeciaRL following the evaluation protocol of recent LMM benchmark on open-world image classification [10]. On this general-purpose benchmark, SpeciaRL achieves state-of-the-art performance on three out of four metrics on both the **fine-grained** and the **very fine-grained** test groups, further validating its advantage against existing methods.

Table 3. In-domain evaluation of the training strategies.

		In-domain								
Dataset	Model	Prediction categorization					Metrics			
		S^+	S	S^-	G	A	W	spec. \uparrow	corr. \uparrow	HM \uparrow
CUB [51]	Qwen2.5VL-7B [4]	0.2%	23.0%	15.9%	48.1%	2.0%	11.0%	0.669	0.890	0.764
	Qwen2.5VL-7B ("Be specific")	0.2%	32.2%	13.7%	35.3%	2.6%	16.1%	0.726	0.839	0.779
	Qwen2.5VL-7B (<i>sft</i>)	0.1%	80.4%	0.7%	0.3%	0.0%	18.5%	0.996	0.815	0.896
	Qwen2.5VL-7B (<i>rft</i>)	1.0%	92.7%	0.0%	0.0%	0.0%	6.3%	1.000	0.937	0.968
	SpeciaRL-7B	0.6%	92.7%	0.0%	0.0%	0.0%	6.7%	1.000	0.933	0.965
	Qwen2.5VL-7B (BoN-64)	1.1%	58.0%	14.1%	26.4%	0.1%	0.3%	0.831	0.997	0.907

As previously specified, training is performed on a subset of CUB [51], implying that the evaluations on the fine-grained and very fine-grained sets are out-of-domain. For completeness, Tab. 3 reports the in-domain evaluation on the CUB test set. In this setting, all training-based variants achieve very high specificity, exceeding BoN-64. In terms of correctness, only the RL-based methods improve over the base model, although they remain below BoN-64. Overall, the best harmonic mean is obtained by the two RL-based approaches, surpassing BoN-64.

Qualitative results. Figure 4 presents the model outputs from the base model and our SpeciaRL. For each sample, we visualize both the generated answer and the associated reasoning trace, together with the prediction category evaluated by the judge LLM. Consistent with the quantitative results, SpeciaRL generally produces more specific and fine-grained predictions than the base model. While both models are able to capture fine visual details in their thinking process, only SpeciaRL uses these details to deduce a fine-grained class, as highlighted in green in the reasoning traces. This suggests that our reinforcement learning strategy not only encourages specificity in the final prediction but also enhances the quality and goal-orientation of the reasoning process itself.

4.2. Ablation studies

To justify the key design choices of our reward, we ablate the impact of the *specificity-aware dynamic reward* and the *number N of online rollouts*. Additionally, we evaluate the advantage of SpeciaRL when applied on *different on-policy RL algorithms*, to test its versatility. We conduct all ablations with Qwen2.5VL-7B, and evaluate with the *fine-grained* set. In the *Supp. Mat.*, we provide additional ablations on training data configurations, covering *diverse training domains*, *dataset sizes*, and *mixed-domain* setups. We also validate the *judge’s robustness* across different models and prompt formulations, and analyze the *sensitivity* of SpeciaRL to LLM-as-a-judge classification errors during training.

Different verifiable rewards settings. We compare our specificity-aware dynamic reward against four different static rewards. Starting from the *rft* baseline “ $S^+ \& S(1)$ ” giving reward 1 to S and S^+ predictions, we give credit to less informative categories with a positive reward matching the specificity score as defined in Eq. (4). As shown in Tab. 4, SpeciaRL achieves the best harmonic mean among all the static-reward variants. Interestingly, the standard binary

Figure 4. Qualitative examples of the think-answer output from the base model Qwen2.5VL-7B and our SpeciaRL, which steers the reasoning traces towards more specific prediction.

Table 4. SpeciaRL against *rft* with different static reward rules. Best in bold.

Model	Prediction categorization					Metrics			
	S^+	S	S^-	G	A	W	spec. \uparrow	corr. \uparrow	HM \uparrow
$S^+ \& S(1)$	4.6%	52.2%	5.0%	16.2%	0.0%	21.5%	0.875	0.785	0.825
$S^+ \& S(1)S^- (0.75)$	4.9%	62.6%	5.6%	10.4%	0.0%	16.4%	0.919	0.836	0.875
$S^+ \& S(1)S^- (0.75)G(0.5)$	3.6%	61.1%	5.1%	17.7%	0.0%	12.6%	0.884	0.874	0.878
$S^+ \& S(1)S^- (0.75)G(0.5)A(0.25)$	1.4%	63.9%	6.7%	11.5%	0.0%	16.5%	0.911	0.835	0.871
SpeciaRL-7B (dynamic reward)	5.6%	63.4%	5.1%	10.7%	0.0%	15.2%	0.920	0.848	0.883

reward “ $S^+ \& S(1)$ ” performs worst compared to the other alternatives, highlighting the importance of rewarding correct predictions that are less informative than the ground-truth.

Impact of best of N rollouts. Table 5 presents the results of varying the number of online rollouts N performed during training. Specifically, we report results for $N = 5, 10, 15$, where $N = 10$ is the default setting in our experiments. Interestingly, increasing the rollouts to $N = 15$ leads to lower specificity and correctness. Similar behavior where smaller group sizes outperform larger ones was reported in a recent study on GRPO [11], which might be due to limitations in batch-based grouping strategies that mix unrelated episodes. With rollouts $N = 5$, the model behaves similarly to $N = 10$, with minor gain in specificity yet minor drop in

Table 5. SpeciaRL with different rollouts size N . Best in **bold**.

N rollouts	Prediction categorization						Metrics		
	S^+	S	S^-	G	A	W	spec. \uparrow	corr. \uparrow	HM \uparrow
5	5.5%	63.6%	5.8%	9.5%	0.0%	15.6%	0.925	0.844	0.883
10	5.6%	63.4%	5.1%	10.7%	0.0%	15.2%	0.920	0.848	0.883
15	4.6%	50.4%	3.7%	22.2%	0.0%	19.0%	0.848	0.810	0.824

Table 6. SpeciaRL compared to static reward r_{ft} across different on-policy RL algorithms. Best in **bold**.

RL method	Prediction categorization						Metrics		
	S^+	S	S^-	G	A	W	spec. \uparrow	corr. \uparrow	HM \uparrow
GRPO [41]	4.6%	52.2%	5.0%	16.2%	0.0%	21.5%	0.875	0.785	0.825
SpeciaRL (GRPO)	5.6%	63.4%	5.1%	10.7%	0.0%	15.2%	0.920	0.848	0.883
Dr.GRPO [33]	8.6%	59.3%	6.5%	5.3%	0.2%	20.1%	0.942	0.799	0.864
SpeciaRL (Dr.GRPO)	6.6%	64.4%	6.0%	4.9%	0.0%	18.2%	0.951	0.818	0.879
DAPO [56]	7.3%	61.0%	7.1%	3.2%	0.4%	21.0%	0.951	0.790	0.862
SpeciaRL (DAPO)	7.2%	64.3%	6.4%	4.4%	0.0%	17.8%	0.952	0.822	0.882

correctness, resulting in equal HM values.

Comparison with RL variants. We compare the standard GRPO [41] algorithm with two recent variants designed to improve token efficiency and training stability, Dr.GRPO [33] and DAPO [56]. As shown in Tab. 6, SpeciaRL consistently increases both specificity and correctness across all three optimizers, and consequently improves HM in every case, with gains ranging from +0.015 (Dr.GRPO) to +0.058 (GRPO). Crucially, these results indicate that our approach is not tied to a single RL formulation: our dynamic reward is *compatible with general online RL frameworks* and transfers robustly across different policy optimization algorithms.

5. Conclusion

We addressed open-world fine-grained classification with reasoning LMMs, aiming to generate more specific predictions without sacrificing correctness. Reasoning LMMs are overly generic in recognizing fine-grained visual concepts. Yet, our analysis showed that this is not because they lack domain knowledge, but because they fail to reliably express the most specific prediction they can produce. We introduced SpeciaRL, a specificity-aware reinforcement learning framework that uses a dynamic, sample-wise reward based on the best predictions found in online rollouts. SpeciaRL leverages a LLM verifier to provide graded feedback enabling specificity-aware dynamic reward within a GRPO-like policy optimization framework. This design promotes specificity within the model’s inherent capability, preventing the correctness degradation observed in existing approaches. Out-of-domain comparisons across fine-grained and very fine-grained benchmarks demonstrate that SpeciaRL consistently achieves the best trade-off between specificity and correctness.

Acknowledgements. This work was supported by the Ministero delle Imprese e del Made in Italy (IPCEI Cloud DM 27

giugno 2022 – IPCEI-CL-0000007). Additional support was provided by the EU Horizon projects SWARMCHESTRATE (No. 101135012) and ELLIOT (No. 101214398). The authors acknowledge the CINECA award under the ISCRA initiative for the availability of high-performance computing resources and support.

References

- [1] Marwa Abdulhai, Isadora White, Charlie Snell, Charles Sun, Joey Hong, Yuexiang Zhai, Kelvin Xu, and Sergey Levine. Lmrl gym: Benchmarks for multi-turn reinforcement learning with language models. *arXiv preprint arXiv:2311.18232*, 2023. 2
- [2] Jean-Baptiste Alayrac, Jeff Donahue, Pauline Luc, Antoine Miech, Iain Barr, Yana Hasson, Karel Lenc, Arthur Mensch, Katherine Millican, Malcolm Reynolds, et al. Flamingo: a visual language model for few-shot learning. *NeurIPS*, 2022. 2
- [3] Shuai Bai, Keqin Chen, Xuejing Liu, Jialin Wang, Wenbin Ge, Sibong Song, Kai Dang, Peng Wang, Shijie Wang, Jun Tang, et al. Qwen2.5-vl technical report. *arXiv preprint arXiv:2502.13923*, 2025. 1, 2, 4, 5, 7
- [4] Shuai Bai, Keqin Chen, Xuejing Liu, Jialin Wang, Wenbin Ge, Sibong Song, Kai Dang, Peng Wang, Shijie Wang, Jun Tang, et al. Qwen2.5-vl technical report. *arXiv preprint arXiv:2502.13923*, 2025. 1, 7, 8, 17, 18
- [5] Abhijit Bendale and Terrance Boulton. Towards open world recognition. In *CVPR*, pages 1893–1902, 2015. 1
- [6] Lukas Bossard, Matthieu Guillaumin, and Luc Van Gool. Food-101—mining discriminative components with random forests. In *ECCV*, 2014. 4, 17, 19, 20
- [7] Zhe Chen, Weiyun Wang, Yue Cao, Yangzhou Liu, Zhangwei Gao, Erfei Cui, Jinguo Zhu, Shenglong Ye, Hao Tian, Zhaoyang Liu, et al. Expanding performance boundaries of open-source multimodal models with model, data, and test-time scaling. *arXiv preprint arXiv:2412.05271*, 2024. 7, 17, 18
- [8] Zhe Chen, Jiannan Wu, Wenhai Wang, Weijie Su, Guo Chen, Sen Xing, Muyan Zhong, Qinglong Zhang, Xizhou Zhu, Lewei Lu, et al. Internvl: Scaling up vision foundation models and aligning for generic visual-linguistic tasks. In *CVPR*, 2024. 1, 2, 7
- [9] Alessandro Conti, Enrico Fini, Massimiliano Mancini, Paolo Rota, Yiming Wang, and Elisa Ricci. Vocabulary-free image classification. *NeurIPS*, 2023. 1, 6, 7, 17, 18
- [10] Alessandro Conti, Massimiliano Mancini, Enrico Fini, Yiming Wang, Paolo Rota, and Elisa Ricci. On large multimodal models as open-world image classifiers. In *ICCV*, 2025. 1, 2, 3, 4, 5, 6, 7, 13, 15, 19, 20
- [11] Bryan LM de Oliveira, Felipe V Frujeri, Marcos PCM Queiroz, Luana GB Martins, Telma W de L Soares, and Luckeciano C Melo. Learning without critics? revisiting gpo in classical reinforcement learning environments. *arXiv preprint arXiv:2511.03527*, 2025. 8
- [12] Jia Deng, Wei Dong, Richard Socher, Li-Jia Li, Kai Li, and Li Fei-Fei. Imagenet: A large-scale hierarchical image database. In *CVPR*, pages 248–255. Ieee, 2009. 1
- [13] Abhimanyu Dubey, Abhinav Jauhri, Abhinav Pandey, Abhishek Kadian, Ahmad Al-Dahle, Aiesha Letman, Akhil Mathur, Alan Schelten, Amy Yang, Angela Fan, et al. The llama 3 herd of models. *arXiv e-prints*, pages arXiv–2407, 2024. 4, 6, 15
- [14] Chaoyou Fu, Peixian Chen, Yunhang Shen, Yulei Qin, Mengdan Zhang, Xu Lin, Jinrui Yang, Xiawu Zheng, Ke Li, Xing Sun, Yunsheng Wu, Rongrong Ji, Caifeng Shan, and Ran He. Mme: A comprehensive evaluation benchmark for multimodal large language models, 2025. 2
- [15] Anisha Gunjal, Anthony Wang, Elaine Lau, Vaskar Nath, Yunzhong He, Bing Liu, and Sean Hendryx. Rubrics as rewards: Reinforcement learning beyond verifiable domains. *arXiv preprint arXiv:2507.17746*, 2025. 3
- [16] Daya Guo, Dejian Yang, Haowei Zhang, Junxiao Song, Ruoyu Zhang, Runxin Xu, Qihao Zhu, Shirong Ma, Peiyi Wang, Xiao Bi, et al. Deepseek-r1: Incentivizing reasoning capability in llms via reinforcement learning. *arXiv preprint arXiv:2501.12948*, 2025. 2, 3, 5, 6
- [17] Binyuan Hui, Jian Yang, Zeyu Cui, Jiaxi Yang, Dayiheng Liu, Lei Zhang, Tianyu Liu, Jiajun Zhang, Bowen Yu, Keming Lu, et al. Qwen2.5-coder technical report. *arXiv preprint arXiv:2409.12186*, 2024. 3
- [18] Aaron Jaech, Adam Kalai, Adam Lerer, Adam Richardson, Ahmed El-Kishky, Aiden Low, Alec Helyar, Aleksander Madry, Alex Beutel, Alex Carney, et al. Openai o1 system card. *arXiv preprint arXiv:2412.16720*, 2024. 2
- [19] Chao Jia, Yinfei Yang, Ye Xia, Yi-Ting Chen, Zarana Parekh, Hieu Pham, Quoc Le, Yun-Hsuan Sung, Zhen Li, and Tom Duerig. Scaling up visual and vision-language representation learning with noisy text supervision. In *ICML*, pages 4904–4916. PMLR, 2021. 2
- [20] Takeshi Kojima, Shixiang Shane Gu, Machel Reid, Yutaka Matsuo, and Yusuke Iwasawa. Large language models are zero-shot reasoners. *NeurIPS*, 35:22199–22213, 2022. 2
- [21] Jonathan Krause, Michael Stark, Jia Deng, and Li Fei-Fei. 3d object representations for fine-grained categorization. In *ICCV-WS*, 2013. 4, 17, 18
- [22] Woosuk Kwon, Zhuohan Li, Siyuan Zhuang, Ying Sheng, Lianmin Zheng, Cody Hao Yu, Joseph Gonzalez, Hao Zhang, and Ion Stoica. Efficient memory management for large language model serving with pagedattention. In *Proceedings of the symposium on operating systems principles*, pages 611–626, 2023. 13, 15
- [23] Nathan Lambert, Jacob Morrison, Valentina Pyatkin, Shengyi Huang, Hamish Ivison, Faeze Brahman, Lester James V Miranda, Alisa Liu, Nouha Dziri, Shane Lyu, et al. Tulu 3: Pushing frontiers in open language model post-training. *arXiv preprint arXiv:2411.15124*, 2024. 3, 5
- [24] J Richard Landis and Gary G Koch. The measurement of observer agreement for categorical data. *biometrics*, 1977. 21
- [25] Bohao Li, Yuying Ge, Yixiao Ge, Guangzhi Wang, Rui Wang, Ruimao Zhang, and Ying Shan. Seed-bench: Benchmarking multimodal large language models. In *CVPR*, 2024. 2
- [26] Bo Li, Kaichen Zhang, Hao Zhang, Dong Guo, Renrui Zhang, Feng Li, Yuanhan Zhang, Ziwei Liu, and Chunyuan Li. Llava-next: Stronger llms supercharge multimodal capabilities in the wild. 2024. 1
- [27] Bo Li, Yuanhan Zhang, Dong Guo, Renrui Zhang, Feng Li, Hao Zhang, Kaichen Zhang, Peiyuan Zhang, Yanwei Li, Ziwei Liu, et al. Llava-onevision: Easy visual task transfer. *arXiv preprint arXiv:2408.03326*, 2024. 2
- [28] Junnan Li, Dongxu Li, Silvio Savarese, and Steven Hoi. Blip-2: Bootstrapping language-image pre-training with frozen

- image encoders and large language models. In *ICML*, 2023. 1, 2
- [29] Kunchang Li, Yali Wang, Yanan He, Yizhuo Li, Yi Wang, Yi Liu, Zun Wang, Jilan Xu, Guo Chen, Ping Luo, et al. Mvbench: A comprehensive multi-modal video understanding benchmark. In *CVPR*, 2024. 2
- [30] Ming Li, Jike Zhong, Shitian Zhao, Yuxiang Lai, and Kaipeng Zhang. Think or not think: A study of explicit thinking in rule-based visual reinforcement fine-tuning. *arXiv preprint arXiv:2503.16188*, 2025. 3, 6
- [31] Huan Liu, Lingyu Xiao, Jiangjiang Liu, Xiaofan Li, Ze Feng, Sen Yang, and Jingdong Wang. Revisiting mllms: An in-depth analysis of image classification abilities. *arXiv preprint arXiv:2412.16418*, 2024. 1, 2
- [32] Yuan Liu, Haodong Duan, Yuanhan Zhang, Bo Li, Songyang Zhang, Wangbo Zhao, Yike Yuan, Jiaqi Wang, Conghui He, Ziwei Liu, et al. Mmbench: Is your multi-modal model an all-around player? In *ECCV*, 2024. 2
- [33] Zichen Liu, Changyu Chen, Wenjun Li, Penghui Qi, Tianyu Pang, Chao Du, Wee Sun Lee, and Min Lin. Understanding r1-zero-like training: A critical perspective. *arXiv preprint arXiv:2503.20783*, 2025. 9
- [34] Ziyu Liu, Zeyi Sun, Yuhang Zang, Xiaoyi Dong, Yuhang Cao, Haodong Duan, Dahua Lin, and Jiaqi Wang. Visual-rft: Visual reinforcement fine-tuning. *arXiv preprint arXiv:2503.01785*, 2025. 3, 6
- [35] Subhransu Maji, Esa Rahtu, Juho Kannala, Matthew Blaschko, and Andrea Vedaldi. Fine-grained visual classification of aircraft. *arXiv preprint arXiv:1306.5151*, 2013. 4, 17, 18
- [36] Maria-Elena Nilsback and Andrew Zisserman. Automated flower classification over a large number of classes. In *Indian conference on computer vision, graphics & image processing*. IEEE, 2008. 4, 17, 19, 20
- [37] Long Ouyang, Jeffrey Wu, Xu Jiang, Diogo Almeida, Carroll Wainwright, Pamela Mishkin, Chong Zhang, Sandhini Agarwal, Katarina Slama, Alex Ray, et al. Training language models to follow instructions with human feedback. *NeurIPS*, 35:27730–27744, 2022. 2, 3
- [38] Omkar M Parkhi, Andrea Vedaldi, Andrew Zisserman, and CV Jawahar. Cats and dogs. In *CVPR*, 2012. 4, 17, 19, 20
- [39] Alec Radford, Jong Wook Kim, Chris Hallacy, Aditya Ramesh, Gabriel Goh, Sandhini Agarwal, Girish Sastry, Amanda Askell, Pamela Mishkin, Jack Clark, et al. Learning transferable visual models from natural language supervision. In *ICML*, 2021. 1, 2, 6
- [40] Lars Schmarje, Monty Santarossa, Simon-Martin Schröder, and Reinhard Koch. A survey on semi-, self-and unsupervised learning for image classification. *IEEE Access*, 9:82146–82168, 2021. 1
- [41] Zhihong Shao, Peiyi Wang, Qihao Zhu, Runxin Xu, Junxiao Song, Xiao Bi, Haowei Zhang, Mingchuan Zhang, YK Li, Yang Wu, et al. Deepseekmath: Pushing the limits of mathematical reasoning in open language models. *arXiv preprint arXiv:2402.03300*, 2024. 2, 3, 6, 9
- [42] Guangming Sheng, Chi Zhang, Zilingfeng Ye, Xibin Wu, Wang Zhang, Ru Zhang, Yanghua Peng, Haibin Lin, and Chuan Wu. Hybridflow: A flexible and efficient rlhf framework. *arXiv preprint arXiv: 2409.19256*, 2024. 6, 15
- [43] Amanpreet Singh, Ronghang Hu, Vedanuj Goswami, Guillaume Couairon, Wojciech Galuba, Marcus Rohrbach, and Douwe Kiela. Flava: A foundational language and vision alignment model. In *CVPR*, 2022. 2
- [44] Vésteinn Snæbjarnarson, Kevin Du, Niklas Stoehr, Serge Belongie, Ryan Cotterell, Nico Lang, and Stella Frank. Taxonomy-aware evaluation of vision-language models. In *CVPR*, pages 9109–9120, 2025. 2, 3
- [45] Nisan Stiennon, Long Ouyang, Jeffrey Wu, Daniel Ziegler, Ryan Lowe, Chelsea Voss, Alec Radford, Dario Amodei, and Paul F Christiano. Learning to summarize with human feedback. *NeurIPS*, 33:3008–3021, 2020. 2, 3
- [46] Yi Su, Dian Yu, Linfeng Song, Juntao Li, Haitao Mi, Zhaopeng Tu, Min Zhang, and Dong Yu. Crossing the reward bridge: Expanding rl with verifiable rewards across diverse domains. *arXiv preprint arXiv:2503.23829*, 2025. 3
- [47] Richard S Sutton, Andrew G Barto, et al. *Reinforcement learning: An introduction*. MIT press Cambridge, 1998. 2
- [48] Yuwen Tan, Yuan Qing, and Boqing Gong. Vision llms are bad at hierarchical visual understanding, and llms are the bottleneck. *arXiv preprint arXiv:2505.24840*, 2025. 2
- [49] Kimi Team, Yifan Bai, Yiping Bao, Guanduo Chen, Jiahao Chen, Ningxin Chen, Ruijue Chen, Yanru Chen, Yuankun Chen, Yutian Chen, et al. Kimi k2: Open agentic intelligence. *arXiv preprint arXiv:2507.20534*, 2025. 3, 5
- [50] Qwen Team. Qwen3 technical report, 2025. 6, 15
- [51] Catherine Wah, Steve Branson, Peter Welinder, Pietro Perona, and Serge Belongie. The caltech-ucsd birds-200-2011 dataset, 2011. 6, 8, 17, 18, 20
- [52] Peng Wang, Shuai Bai, Sinan Tan, Shijie Wang, Zhihao Fan, Jinze Bai, Keqin Chen, Xuejing Liu, Jialin Wang, Wenbin Ge, et al. Qwen2-vl: Enhancing vision-language model’s perception of the world at any resolution. *arXiv preprint arXiv:2409.12191*, 2024. 2
- [53] Jason Wei, Xuezhi Wang, Dale Schuurmans, Maarten Bosma, Fei Xia, Ed Chi, Quoc V Le, Denny Zhou, et al. Chain-of-thought prompting elicits reasoning in large language models. *NeurIPS*, 35:24824–24837, 2022. 2
- [54] An Yang, Beichen Zhang, Binyuan Hui, Bofei Gao, Bowen Yu, Chengpeng Li, Dayiheng Liu, Jianhong Tu, Jingren Zhou, Junyang Lin, et al. Qwen2. 5-math technical report: Toward mathematical expert model via self-improvement. *arXiv preprint arXiv:2409.12122*, 2024. 3
- [55] Huaiyuan Ying, Shuo Zhang, Linyang Li, Zhejian Zhou, Yunfan Shao, Zhaoye Fei, Yichuan Ma, Jiawei Hong, Kuikun Liu, Ziyi Wang, et al. Internlm-math: Open math large language models toward verifiable reasoning. *arXiv preprint arXiv:2402.06332*, 2024. 3
- [56] Qiyang Yu, Zheng Zhang, Ruofei Zhu, Yufeng Yuan, Xiaochen Zuo, Yu Yue, Weinan Dai, Tiantian Fan, Gaohong Liu, Lingjun Liu, et al. Dapo: An open-source llm reinforcement learning system at scale. *arXiv preprint arXiv:2503.14476*, 2025. 9
- [57] Kaiyu Yue, Bor-Chun Chen, Jonas Geiping, Hengduo Li, Tom Goldstein, and Ser-Nam Lim. Object recognition as next token prediction. In *CVPR*, 2024. 2

- [58] Yang Yue, Zhiqi Chen, Rui Lu, Andrew Zhao, Zhaokai Wang, Shiji Song, and Gao Huang. Does reinforcement learning really incentivize reasoning capacity in llms beyond the base model? *arXiv preprint arXiv:2504.13837*, 2025. [5](#)
- [59] Eric Zelikman, Yuhuai Wu, Jesse Mu, and Noah D Goodman. Star: Self-taught reasoner bootstrapping reasoning with reasoning. In *NeurIPS*, 2024. [7](#)
- [60] Xiaohua Zhai, Basil Mustafa, Alexander Kolesnikov, and Lucas Beyer. Sigmoid loss for language image pre-training. In *ICCV*, 2023. [1](#), [2](#)
- [61] Kechi Zhang, Ge Li, Yihong Dong, Jingjing Xu, Jun Zhang, Jing Su, Yongfei Liu, and Zhi Jin. Codedpo: Aligning code models with self generated and verified source code. In *ACL*, pages 15854–15871, 2025. [3](#)
- [62] Ruohong Zhang, Bowen Zhang, Yanghao Li, Haotian Zhang, Zhiqing Sun, Zhe Gan, Yinfei Yang, Ruoming Pang, and Yiming Yang. Improve vision language model chain-of-thought reasoning. In *ACL*, pages 1631–1662, 2025. [7](#)
- [63] Yuhui Zhang, Alyssa Unell, Xiaohan Wang, Dhruva Ghosh, Yuchang Su, Ludwig Schmidt, and Serena Yeung-Levy. Why are visually-grounded language models bad at image classification? *NeurIPS*, 2024. [1](#), [2](#)
- [64] Yuhui Zhang, Yuchang Su, Yiming Liu, Xiaohan Wang, James Burgess, Elaine Sui, Chenyu Wang, Josiah Aklilu, Alejandro Lozano, Anjiang Wei, et al. Automated generation of challenging multiple-choice questions for vision language model evaluation. In *CVPR*, pages 29580–29590, 2025. [2](#)
- [65] Deyao Zhu, Jun Chen, Xiaoqian Shen, Xiang Li, and Mohamed Elhoseiny. Minigpt-4: Enhancing vision-language understanding with advanced large language models. In *ICLR*, 2024. [1](#), [2](#)
- [66] Yuxin Zuo, Kaiyan Zhang, Li Sheng, Shang Qu, Ganqu Cui, Xuekai Zhu, Haozhan Li, Yuchen Zhang, Xinwei Long, Ermo Hua, et al. Ttrl: Test-time reinforcement learning. *arXiv preprint arXiv:2504.16084*, 2025. [2](#)

Specificity-aware reinforcement learning for fine-grained open-world classification

Supplementary Material

In this supplementary material, we present additional details and analyses that complement the content of the main document. First, in Sec. A, we provide further implementation details, including the prompts we used for the LMM and the LLM verifier, along with the optimization strategies adopted to improve training efficiency. Next, in Sec. B, we report the complete out-of-domain evaluation results for each individual dataset in both fine-grained and very fine-grained sets, along with further prompting baselines and additional qualitative examples. Finally, in Sec. B.4, we extend the ablation studies on the impact of training sets from different domains and the training-set size on the performance of SpeciaRL.

A. Additional implementation details

A.1. Prompts

Here, we report all the prompts used in our experiments. These include the classification prompt P_c provided to the reasoning LMM Φ_{LMM}^θ , the verification prompt P_j used by the LLM-as-a-judge Ψ_{LLM} , and the prompt used to generate the reasoning traces for the supervised fine-tuning (*sft*) baseline.

A.1.1. LMM prompts

In our experiments, we consider a total of three different prompts when querying a LMM to classify an image.

Default. Our default prompt is shown in Fig. 5. Since our work focuses on reasoning models, we not only request a classification of the input image, but we also explicitly instruct the model to first perform reasoning and then provide a single label. Specifically, we follow the standard `<think>/<answer>` tags format. This structured output simplifies the extraction of the final prediction and its subsequent verification by the LLM-as-a-judge.

“Be specific”. In the “Be specific” baseline, we explicitly encourage the model to be specific in its prediction. To this end, we modify the default prompt by adding the requirement to be specific. The complete text query is reported in Fig. 6.

Format free. When considering the evaluation protocol in [10], for consistency and fair comparison, we adopt the same prompting strategy reported in the original paper [10], as shown in Fig. 7. Since this previous work does not have a focus on reasoning models, it adopts a more general-purpose prompt without formatting requirements.

A.1.2. LLM-as-a-judge prompt

Figure 8 shows the prompt used when querying the LLM verifier to categorize a prediction into the categories defined in the main paper. This prompt provides a precise definition with in-context examples for each category. The

Default LMM prompt (P_c)

Classify the image.
Output the thinking process in `<think>` `</think>` and the final answer in `<answer>` `</answer>` tags.
The output answer format should be as follows:
`<think>` ... `</think>` `<answer>`a single label or the word ‘None’ to abstain.`</answer>`.
Please strictly follow the format.

Figure 5. LMM default prompt for prediction.

“Be specific” LMM prompt (P_c)

Classify the image, **be specific**.
Output the thinking process in `<think>` `</think>` and the final answer in `<answer>` `</answer>` tags.
The output answer format should be as follows:
`<think>` ... `</think>` `<answer>`a single label or the word ‘None’ to abstain.`</answer>`.
Please strictly follow the format.

Figure 6. LMM prompt for prediction for the “Be specific” baseline.

Format free LMM prompt (P_c) [10]

What type of object is in this photo?

Figure 7. LMM prompt used in the evaluation protocol of [10].

placeholder `%s` is replaced with the actual `ground_truth` and `prediction` formatted in the specified JSON format. To eliminate the possibility of invalid responses from the LLM verifier, we utilize the vLLM [22] guided decoding strategy to constrain the model in generating only one of the predefined categories as the response.

A.1.3. CoT generation prompt

Figure 9 reports the prompt used to generate a chain-of-thought reasoning trace for each sample in the training set, which are then used to construct the custom dataset for supervised fine-tuning. This prompt provides the LMM with the ground-truth label associated to the image, and requests a thinking trace leading to the correct prediction.

A.2. Optimizations

Our study can be computationally demanding at training and evaluation due to the LMM inference and LLM-as-a-judge evaluation. We therefore adopt several optimizations strategies to reduce computational costs.

LLM-as-a-judge prompt (P_j)

Role: You are an expert AI classifier. Your goal is to classify a model's prediction against a ground_truth label.

Task: You will receive a single JSON object. Your output must be **only the classification category** and nothing else.

Classification Categories

- **Specific:** The prediction is an exact match or a direct synonym for the ground truth. This includes common name/scientific name equivalence.

prediction: "Panthera leo" groundtruth: "lion"

prediction: "passiflora" groundtruth: "passion flower"

- **Less Specific:** The prediction is a correct, but **closely related parent category** (e.g., family, genus, product line) of the ground truth.

prediction: "Warbler" groundtruth: "Golden-winged Warbler"

prediction: "Boeing 707" groundtruth: "707-320"

- **Generic:** The prediction is correct, but a **significantly broader category** than the ground truth.

prediction: "dog" groundtruth: "samoyed"

prediction: "Commercial Airline" groundtruth: "757-200"

- **More Specific:** The prediction is a correct, but **more specific subtype or instance** of the ground truth.

prediction: "samoyed" groundtruth: "dog"

prediction: "757-200" groundtruth: "Commercial Airline"

- **Wrong:** The prediction is factually incorrect, contradictory, malformed, completely unrelated to the ground truth, or contains multiple options.

prediction: "cat" groundtruth: "dog"

prediction: "Blue-winged Warbler" groundtruth: "Golden-winged Warbler"

prediction: "blrld" groundtruth: "bird"

prediction: "robin or cardinal" groundtruth: "bird"

prediction: "_prototype" groundtruth: "Boeing 717"

- **Abstain:** The prediction is a refusal to answer.

prediction: "none"

prediction: "I don't know"

prediction: "Cannot tell"

Input Format: You will receive a single JSON object with the following structure:

```
{"ground_truth": "<the_ground_truth_label>","prediction": "<the_vlm_prediction>"}
```

Output Format: Your response must be a **single word** representing the classification category.

Prompt:

Classify the prediction in the following JSON object based on the rules provided. Your output must be a single word.

INPUT:

%s

Figure 8. Prompt for the LLM-as-a-judge verifier categorizing a prediction given the target ground-truth.

CoT generation prompt

Given the image and the correct classification label: {ground_truth}.
Generate a correct well-reasoned response that will answer the following question:

Classify the image.

Output the thinking process in `<think>` `</think>` and the final answer in `<answer>` `</answer>` tags.

The output answer format should be as follows: `<think>` ... `</think>` `<answer>` a single label or the word 'None' to abstain. `</answer>`.

Please strictly follow the format.

Describe the content of the image, then infer the correct classification label. The thinking process must proceed without assuming or referencing the true label in advance. Use the correct classification label in the final answer and strictly follow the format.

Figure 9. Prompt for generating the reasoning traces used to train the supervised fine-tuning baseline model.

Inference Engine. In our experiments, we used the vLLM [22] inference engine both to generate the LMM predictions and to compute the LLM-as-a-judge categorization. This engine is highly optimized and enabled a significant speed-up of the evaluation process. Among its key features, it includes PagedAttention [22] for efficient memory management, continuous batching, which is crucial in our setting where variable-size image inputs make static batch selection difficult, and prefix caching, which is beneficial since our textual prompt is mostly fixed. For instance, generating 1000 predictions for Flowers102 with Qwen2.5-VL-7B on a A100 64 GB GPU takes 2.27 minutes with vLLM. In comparison, a naive PyTorch implementation requires 25.11 minutes, using a batch size of 32, which is the largest batch size avoiding out-of-memory errors across all our evaluation datasets. The PyTorch implementation incurs computation time that is a magnitude higher than using vLLM. Only when following the evaluation protocol in [10], we used the same testing code provided by the authors, which is built on PyTorch.

LLM-as-a-judge optimization via caching. We implemented a caching mechanism to reduce the verification time of the LLM-as-a-judge categorization procedure. This system stores a dictionary where (prediction, ground_truth) pairs are associated to the corresponding verification_category. This avoids repeating the LLM verification of a pair that has already been categorized in a previous computation. The cached data is persistent, allowing results to be reused across different runs. We used this cache-based solution to speed up the categorization process both during evaluation and during the reward computation in RL training. During evaluation, we run Llama-3-72B [13] using vLLM with tensor parallelism set to 4, distributing the model across four A100 GPUs. For a test subsample of 1000 predictions from Flowers102, our optimized implementation, with an initially empty cache, completes verification in 6.77 seconds, with only 301 actual

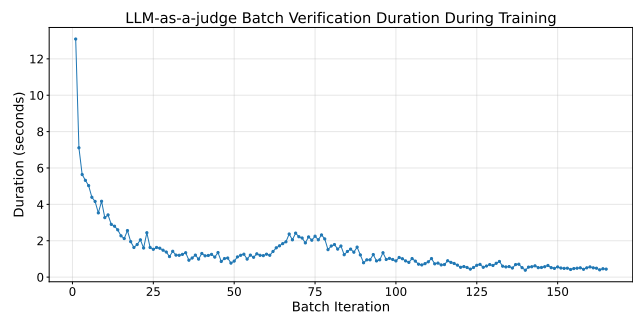


Figure 10. LLM-as-a-judge per-batch verification times during reinforcement learning training, showing the speedup obtained as cache hit rates increase when starting from an empty cache.

LLM calls and a 70% cache hit rate. During reinforcement learning, we use a total of six A100 GPUs: one four-GPU node running the training loop with verl (an open source implementation of [42]) and two additional GPUs on a separate node performing batched LLM-as-a-judge inference using Qwen3-30B-A3B-Instruct-2507-FP8 [50] with tensor parallelism set to 2. With a batch size of 256 and 10 rollouts, each verification batch contains 2560 predictions. Analyzing the reward calculation durations shown in Fig. 10, we see an initial warm-up phase in which early batches require 2-14 seconds while the cache is being populated. Afterwards, the processing time quickly drops and stabilizes at approximately 0.5 to 1 seconds per batch, except for a mid-training bump that may be caused by cache misses caused by the model exploration. Overall, reinforcement learning training takes approximately 12 hours using our optimized implementation.

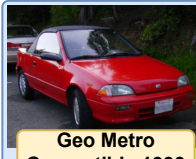
 <p>Stemless Gentian</p>	<p>Qwen2.5VL-7B Answer: Gentiana S⁻</p> <p>Thinking: The image shows a single blue flower with a bell-like shape, growing in a grassy area. The flower appears to be a Gentiana, a genus of flowering plants in the family Gentianaceae, known for their vibrant colors and often found in alpine or mountainous regions. The surrounding vegetation and the flower's structure are consistent with this identification.</p>	 <p>Magnolia</p>	<p>Qwen2.5VL-7B Answer: Magnolia S</p> <p>Thinking: The image shows a white flower with six petals, which is characteristic of a star magnolia. The flower is in full bloom, and the background consists of branches and buds, suggesting it is part of a tree. The flower's structure and color are distinct and easily identifiable.</p>
<p>SpeciaRL Answer: Gentiana Acaulis S</p> <p>Thinking: The image shows a single flower with a deep blue color, which is characteristic of <i>Gentiana acaulis</i>, commonly known as the alpine gentian. The flower is surrounded by green foliage, which is typical of alpine plants. The flower's structure, with its five petals and the way it is growing, is consistent with the appearance of this species.</p>	<p>SpeciaRL Answer: Magnolia Stellata S⁺</p> <p>Thinking: The image shows a white flower with six petals, which is characteristic of a star magnolia (<i>Magnolia stellata</i>). The flower is in full bloom, and the surrounding branches and buds suggest it is part of a tree. The petals are large and white, and the center of the flower is green, which is typical for this species.</p>		
 <p>Greek Salad</p>	<p>Qwen2.5VL-7B Answer: Salad G</p> <p>Thinking: The image shows a plate of food that appears to be a salad. The salad includes ingredients such as lettuce, tomato slices, cucumber slices, feta cheese, and an olive. The presentation suggests a fresh and healthy meal.</p>	 <p>Ravioli</p>	<p>Qwen2.5VL-7B Answer: Pasta Dish G</p> <p>Thinking: The image shows a close-up of a dish that appears to be ravioli, a type of pasta, covered in a creamy sauce and garnished with what looks like sage leaves. The dish is likely a type of pasta dish, possibly a ravioli al burro e sale (butter and salt ravioli) or a similar variation. The presence of sage leaves suggests a savory and possibly Italian-inspired dish.</p>
<p>SpeciaRL Answer: Greek Salad S</p> <p>Thinking: The image shows a plate of food that appears to be a salad. The salad includes ingredients such as lettuce, tomato slices, cucumber slices, feta cheese, and an olive. The dish is garnished with a sprinkle of what looks like crumbled feta cheese on top. The presentation and ingredients suggest a fresh and healthy meal, possibly a Greek salad.</p>	<p>SpeciaRL Answer: Ravioli S</p> <p>Thinking: The image shows a close-up of a dish that appears to be ravioli, a type of pasta, covered in a creamy sauce and garnished with what looks like sage leaves. The dish is likely a type of ravioli alla Romana, a traditional Italian dish. The presence of sage leaves and the creamy sauce suggest a savory and possibly herbaceous flavor profile.</p>		
 <p>Wheaten Terrier</p>	<p>Qwen2.5VL-7B Answer: Dog G</p> <p>Thinking: The image shows a close-up of a dog with a light-colored, shaggy coat. The dog appears to be a breed with a distinctive facial structure and a friendly expression. The dog's fur is thick and appears to be well-groomed. The dog's eyes are dark and expressive, and its mouth is slightly open, revealing its teeth. The overall appearance suggests that the dog is a breed known for its friendly and affectionate nature.</p>	 <p>Basset Hound</p>	<p>Qwen2.5VL-7B Answer: Basset Hound S</p> <p>Thinking: The image shows a dog, specifically a Basset Hound, lying on a carpet in a living room setting. The dog has long ears, a white chest, and a black and brown coat. The background includes a fireplace and shelves with various items.</p>
<p>SpeciaRL Answer: Soft Coated Wheaten Terrier S⁺</p> <p>Thinking: The image shows a close-up of a dog with a light-colored, shaggy coat. The dog appears to be a Soft Coated Wheaten Terrier, identifiable by its distinctive facial features and coat texture. The dog's expression is relaxed, with its mouth slightly open, showing its teeth. The breed is known for its friendly and energetic nature.</p>	<p>SpeciaRL Answer: Basset Hound S</p> <p>Thinking: The image shows a dog with long ears, a white chest, and a black and brown coat, which are characteristic features of a Basset Hound. The setting appears to be a home interior, with a fireplace and shelves in the background. The dog is lying on a patterned rug, looking directly at the camera.</p>		
 <p>DHC-6</p>	<p>Qwen2.5VL-7B Answer: Seaplane G</p> <p>Thinking: The image shows a seaplane with the text "MALDIVIAN AIR TAXI" on its side, indicating it is used for air taxi services. The plane is on water, which is typical for seaplanes, and the registration number "8Q-MAP" is visible. The setting appears to be a tropical location, possibly the Maldives, given the name on the plane.</p>	 <p>737-900</p>	<p>Qwen2.5VL-7B Answer: Aircraft G</p> <p>Thinking: The image shows an airplane with the livery of Alaska Airlines, which is a well-known airline. The aircraft is a Boeing 737, identifiable by its size, shape, and the number of engines. The image is taken on a tarmac, suggesting it is either preparing for takeoff or has just landed. The presence of the Alaska Airlines logo and the aircraft's registration number (N306AS) confirm the identity of the aircraft.</p>
<p>SpeciaRL Answer: DHC-6 Twin Otter S</p> <p>Thinking: The image shows a seaplane with the livery of "Maldivian Air Taxi." The aircraft is a de Havilland Canada DHC-6 Twin Otter, a popular model used for short-haul flights, particularly in remote areas. The registration number "8Q-MAP" is visible on the fuselage, and the aircraft is equipped with floats, indicating it is designed for operation on water. The setting appears to be a tropical location, likely the Maldives, given the livery and the environment.</p>	<p>SpeciaRL Answer: Boeing 737 S⁻</p> <p>Thinking: The image shows a commercial airplane on a tarmac. The livery on the aircraft indicates it belongs to Alaska Airlines, as seen from the logo and the name "Alaska" written on the fuselage. The aircraft is a Boeing 737, identifiable by its size, shape, and the design of the engines and wings. The registration number "N306AS" is visible on the rear of the aircraft.</p>		
 <p>Bentley Continental GT Coupe 2012</p>	<p>Qwen2.5VL-7B Ans: Luxury Sports Car G</p> <p>Thinking: The image shows a sleek, silver sports car with a low profile and a streamlined body. The car has a coupe body style with a long hood and short rear deck, which is typical of high-performance sports cars. The wheels are large and have a multi-spoke design, and the car has a modern and elegant appearance. The overall design and features suggest it is a high-end vehicle, likely a concept or production model from a luxury car manufacturer.</p>	 <p>Geo Metro Convertible 1993</p>	<p>Qwen2.5VL-7B Ans: Convertible Car G</p> <p>Thinking: The image shows a red convertible car with a soft top, likely a Ford Escort or a similar model, parked on a street. The car has a sleek design with a sporty appearance, and the setting appears to be a residential area with greenery in the background.</p>
<p>SpeciaRL Answer: Bentley Continental GT S⁻</p> <p>Thinking: The image shows a sleek, silver sports car with a coupe design, featuring a low profile and a streamlined body. The car has a modern and luxurious appearance, with a prominent grille and alloy wheels. The design suggests it is a high-end vehicle, likely a Bentley Continental GT, given the style and features.</p>	<p>SpeciaRL Answer: Geo Metro S⁻</p> <p>Thinking: The image shows a red convertible car with a soft top, likely a Geo Metro, which is a compact car produced by General Motors. The car has a sleek design with a sporty appearance, and it is parked on a street with a natural background. The car's design and features are consistent with the Geo Metro models produced in the 1990s.</p>		

Figure 11. Additional qualitative examples of the think-answer output of the base model Qwen2.5VL-7B and SpeciaRL.

		Fine-grained									
Dataset	Model	Prediction categorization						Metrics			
		S^+	S	S^-	G	A	W	spec. \uparrow	corr. \uparrow	HM \uparrow	
Flowers102 [36]	CaSED [9]	0.0%	57.4%	8.4%	14.7%	0.0%	19.4%	0.883	0.806	0.842	
	InternVL2.5-4B [7]	0.2%	15.8%	1.8%	29.8%	20.0%	32.4%	0.551	0.676	0.607	
	InternVL2.5-8B [7]	0.4%	26.4%	3.3%	15.1%	13.2%	41.6%	0.688	0.584	0.632	
	Qwen2.5VL-3B [4]	0.1%	26.6%	2.7%	49.6%	1.9%	19.2%	0.668	0.808	0.731	
	Qwen2.5VL-7B [4]	0.1%	47.2%	4.1%	34.8%	1.2%	12.7%	0.779	0.873	0.823	
	Qwen2.5VL-7B (“Be specific”)	0.2%	63.5%	5.8%	12.7%	3.0%	14.7%	0.882	0.853	0.867	
	Qwen2.5VL-7B (<i>sft</i>)	1.3%	69.6%	8.5%	3.0%	0.0%	17.5%	0.956	0.825	0.885	
	Qwen2.5VL-7B (<i>rft</i>)	10.4%	70.3%	5.4%	1.5%	0.0%	12.4%	<u>0.976</u>	<u>0.876</u>	<u>0.923</u>	
	SpeciaRL-7B	13.6%	69.2%	5.0%	1.7%	0.0%	10.5%	0.976	0.895	0.934	
	Qwen2.5VL-7B (<i>BoN-64</i>)	4.4%	78.3%	3.7%	9.9%	0.6%	3.1%	0.935	0.969	0.952	
Food101 [6]	CaSED [9]	0.0%	33.0%	13.2%	35.3%	0.0%	18.5%	0.743	0.815	0.777	
	InternVL2.5-4B [7]	0.5%	10.5%	1.4%	71.4%	2.6%	13.7%	0.560	0.863	0.680	
	InternVL2.5-8B [7]	0.8%	10.6%	1.5%	46.3%	30.2%	10.7%	0.483	0.893	0.627	
	Qwen2.5VL-3B [4]	1.5%	17.9%	2.5%	53.4%	7.8%	16.9%	0.601	0.831	0.697	
	Qwen2.5VL-7B [4]	1.3%	32.0%	3.8%	47.8%	2.0%	13.2%	0.697	<u>0.868</u>	0.773	
	Qwen2.5VL-7B (“Be specific”)	1.8%	38.0%	4.6%	34.7%	5.6%	15.3%	0.732	0.847	0.785	
	Qwen2.5VL-7B (<i>sft</i>)	3.5%	51.4%	9.1%	11.6%	0.5%	24.0%	<u>0.889</u>	0.760	<u>0.820</u>	
	Qwen2.5VL-7B (<i>rft</i>)	3.2%	52.0%	7.4%	8.7%	0.1%	28.6%	0.912	0.714	0.801	
	SpeciaRL-7B	1.2%	54.3%	5.8%	19.7%	0.0%	18.9%	0.860	0.811	0.835	
	Qwen2.5VL-7B (<i>BoN-64</i>)	15.1%	52.1%	5.5%	26.5%	0.5%	0.2%	0.849	0.998	0.917	
OxfordPets [38]	CaSED [9]	0.0%	40.7%	10.2%	22.5%	0.0%	26.5%	0.812	0.735	0.772	
	InternVL2.5-4B [7]	0.1%	7.9%	1.3%	61.8%	2.6%	26.2%	0.550	0.738	0.630	
	InternVL2.5-8B [7]	0.9%	13.2%	5.2%	30.6%	18.7%	31.5%	0.554	0.685	0.613	
	Qwen2.5VL-3B [4]	0.8%	7.4%	2.9%	57.3%	3.1%	28.6%	0.557	0.714	0.626	
	Qwen2.5VL-7B [4]	2.7%	35.1%	5.2%	35.6%	1.0%	20.4%	0.751	0.796	0.773	
	Qwen2.5VL-7B (“Be specific”)	4.3%	45.8%	8.2%	19.7%	1.6%	20.4%	0.835	0.796	0.815	
	Qwen2.5VL-7B (<i>sft</i>)	2.4%	72.1%	5.3%	3.2%	0.4%	16.5%	0.961	<u>0.835</u>	0.894	
	Qwen2.5VL-7B (<i>rft</i>)	0.3%	34.7%	2.1%	39.0%	0.0%	23.8%	0.737	0.762	0.749	
	SpeciaRL-7B	2.1%	66.6%	4.5%	10.7%	0.0%	16.1%	<u>0.923</u>	0.839	<u>0.879</u>	
	Qwen2.5VL-7B (<i>BoN-64</i>)	12.9%	59.8%	5.8%	19.5%	0.5%	1.4%	0.882	0.986	0.931	

Table 7. Results on the individual datasets composing the fine-grained set.

B. Additional experimental analysis

We present the per-dataset evaluation of our method, additional qualitative examples, additional prompting baseline results and extended ablation studies.

B.1. Per-dataset evaluation

In the main paper, we reported results averaged over the *fine-grained* and the *very fine-grained* test sets. Here, we present the results for each individual dataset, with Tab. 7 corresponding to the fine-grained ones and Tab. 8 to the very fine-grained ones. Considering overall performance, measured by the harmonic mean (HM), our SpeciaRL achieves the best performance on three out of five benchmarks (Flowers102, Food101, FGVAircraft) and the second best on the remaining two (OxfordPets, StanfordCars). Notably, on three datasets (Flowers102, OxfordPets, StanfordCars), our method not only improves specificity relatively to the base

model, but also correctness. Overall, SpeciaRL performs strongly on all evaluation benchmarks, even though these datasets span domains significantly different from CUB [51], which is used for training. These results support the effectiveness of our method in eliciting a general classification behavior oriented towards both specificity and correctness.

B.2. Additional qualitative results

We showcase additional qualitative classification outputs, two per test dataset, in Fig. 11. Examples in the same row are sampled from the same dataset, ordered from top to bottom as follows: Flowers102 [36], Food101 [6], OxfordPets [38], FGVAircraft [35], and StanfordCars [21]. In line with our quantitative evaluation, our SpeciaRL consistently produces more specific classifications than the base model Qwen2.5VL-7B. The reasoning traces of SpeciaRL contain frequent reference to fine-grained visual evidences that sup-

Very fine-grained										
Dataset	Model	Prediction categorization					Metrics			
		S^+	S	S^-	G	A	W	spec. \uparrow	corr. \uparrow	HM \uparrow
FGVCAircraft [35]	CaSED [9]	0.0%	1.6%	13.9%	37.7%	0.0%	46.8%	0.580	0.532	0.555
	InternVL2.5-4B [7]	0.0%	0.0%	0.2%	66.0%	8.5%	25.3%	0.472	0.747	0.579
	InternVL2.5-8B [7]	0.1%	2.2%	1.3%	59.1%	13.0%	24.4%	0.476	0.756	0.584
	Qwen2.5VL-3B [4]	0.2%	1.6%	1.4%	82.4%	0.3%	14.1%	0.514	0.859	0.643
	Qwen2.5VL-7B [4]	0.1%	6.6%	5.4%	80.7%	0.5%	6.7%	0.549	0.933	0.691
	Qwen2.5VL-7B (“Be specific”)	0.5%	23.0%	20.8%	40.4%	1.2%	14.0%	0.693	<u>0.860</u>	0.768
	Qwen2.5VL-7B (<i>sft</i>)	1.0%	42.9%	33.4%	2.3%	0.1%	20.2%	0.879	0.798	<u>0.837</u>
	Qwen2.5VL-7B (<i>rft</i>)	2.2%	45.9%	25.0%	2.0%	0.0%	25.0%	0.904	0.750	0.820
	SpeciaRL-7B	1.9%	46.5%	29.0%	1.7%	0.0%	20.9%	<u>0.897</u>	0.791	0.841
	Qwen2.5VL-7B (<i>BoN-64</i>)	3.4%	48.9%	24.6%	22.9%	0.1%	0.1%	0.823	0.999	0.903
StanfordCars [21]	CaSED [9]	0.0%	0.2%	13.7%	74.3%	0.0%	11.8%	0.540	0.882	0.669
	InternVL2.5-4B [7]	0.0%	0.1%	2.3%	59.4%	2.6%	35.6%	0.499	0.644	0.563
	InternVL2.5-8B [7]	0.0%	0.2%	10.2%	50.0%	18.2%	21.4%	0.476	0.786	0.593
	Qwen2.5VL-3B [4]	0.0%	0.5%	6.3%	67.8%	4.6%	20.8%	0.509	0.792	0.619
	Qwen2.5VL-7B [4]	0.0%	1.3%	20.1%	68.4%	0.8%	9.4%	0.561	0.906	0.693
	Qwen2.5VL-7B (“Be specific”)	0.1%	2.1%	37.8%	50.8%	1.3%	8.0%	0.611	0.920	0.734
	Qwen2.5VL-7B (<i>sft</i>)	0.0%	2.1%	68.1%	21.2%	0.1%	8.4%	0.698	0.916	0.792
	Qwen2.5VL-7B (<i>rft</i>)	0.2%	3.5%	82.8%	5.0%	0.0%	8.5%	0.746	0.915	0.822
	SpeciaRL-7B	0.2%	3.8%	79.4%	8.4%	0.0%	8.2%	<u>0.738</u>	<u>0.918</u>	<u>0.818</u>
	Qwen2.5VL-7B (<i>BoN-64</i>)	0.5%	12.4%	60.6%	26.3%	0.0%	0.3%	0.716	0.997	0.834

Table 8. Individual dataset results on the very fine-grained set

port the final prediction or the intermediate reasoning process (highlighted in green). The base model (Qwen2.5VL-7B) exhibits such behavior more rarely. Interestingly, we observe cases where the base model identifies a more specific label during the reasoning process (highlighted in yellow), yet outputs a more generic label as the final prediction. This observation further supports our hypothesis that the base model does possess the knowledge and reasoning capabilities to be more precise, however it is biased towards more generic predictions.

We also investigate failure cases of SpeciaRL and report some qualitative examples in Fig. 12. Although our training strategy aims to increase specificity without sacrificing correctness, we find instances where our SpeciaRL makes Wrong predictions when attempting to be specific in its classification (see Top & Center examples in the figure). Also, we notice that SpeciaRL sometimes uses scientific names even when referring to generic concepts. For example, we found it predicts “*Felis Catus*” or “*Canis Lupus Familiaris*” instead of “*Cat*” or “*Dog*” (see Bottom example in the figure). While these predictions are unusual, the LLM verifier correctly categorizes them as Generic. We hypothesize that this interesting behavior could be inherited from training on the CUB [51] bird-species dataset, where the model is positively rewarded for specific scientific names.

	Fine-grained			Very fine-grained		
	spec. \uparrow	corr. \uparrow	HM \uparrow	spec. \uparrow	corr. \uparrow	HM \uparrow
P_c (“Be specific”)	0.816	0.832	0.822	0.652	0.89	0.751
P_c (v1)	0.840	0.830	0.834	0.688	0.885	0.772
P_c (v2)	0.814	0.849	0.830	0.637	0.902	0.746
P_c (v3)	0.884	0.764	0.819	0.777	0.832	0.799

Table 9. Performance comparison of additional prompting baseline.

B.3. Additional Prompting baselines

We report the performance of three additional top-performing variants of the P_c prompt. These variants were generated using ChatGPT by requesting three different optimal predictor prompts given the full task context. As shown in Tab. 9, while performance varies across prompt designs, the overall impact is less significant compared to the gains achieved by the training-based methods reported in the main paper. The full text for these variants is provided in Prompts 13, 14, and 15.

B.4. Additional ablation studies

In this section, we provide the extended ablation studies and robustness checks as outlined in the main paper. Specifically, we analyze training-data configurations for SpeciaRL, varying the training domain, dataset scale, and mixed-domain setups. Finally, we validate the LLM-as-a-judge through agreement analyses across different models and judge-prompt variants, and we assess training sensitivity to injected judge

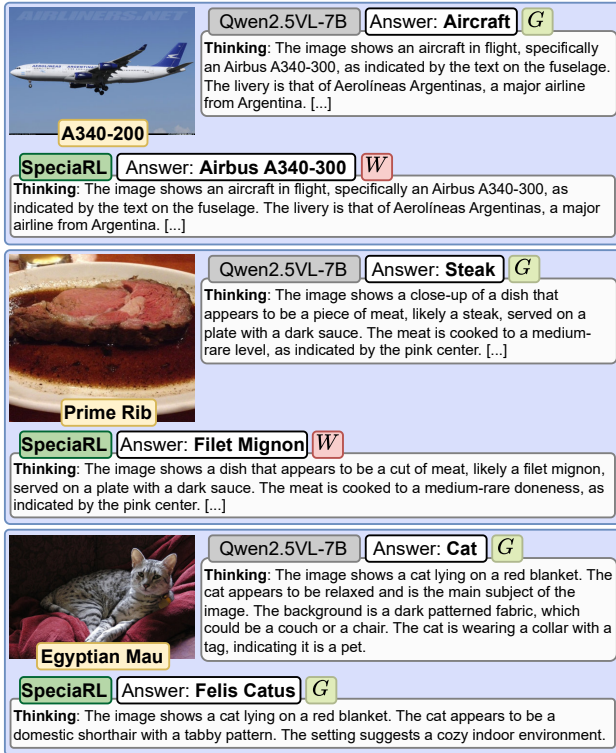


Figure 12. **Failure cases.** Qualitative examples of SpeciaRL providing a Wrong prediction (Top & Center) and of SpeciaRL unnecessarily using a scientific name for a generic concept (Bottom).

Additional LMM prompt (P_c (v1))

Classify the image.
 Prioritize correctness first. Be as specific as you can ONLY when you are confident the finer-grained label is correct. If you are not confident about a fine-grained label, output a more general but correct label instead. If you cannot provide a correct label, output 'None'.
 Output the thinking process in `<think>` `</think>` and the final answer in `<answer>` `</answer>` tags.
 The output answer format should be as follows: `<think>` ... `</think>` `<answer>`a single label or the word 'None' to abstain.`</answer>`.
 Please strictly follow the format.

Figure 13. Generated LMM prompt (P_c (v1)).

classification errors.

B.4.1. training-data configurations

Impact of training set domain. To evaluate how the choice of training data affects SpeciaRL, we independently train three models, each one using a different dataset from the fine-

Additional LMM prompt (P_c (v2))

Classify the image.
 Optimize for high precision: do not guess. If you are unsure, abstain with 'None'. Only output a label when you can justify it from clear visual evidence in the image. When you do output a label, make it the most specific label that the evidence supports.
 Output the thinking process in `<think>` `</think>` and the final answer in `<answer>` `</answer>` tags.
 The output answer format should be as follows: `<think>` ... `</think>` `<answer>`a single label or the word 'None' to abstain.`</answer>`.
 Please strictly follow the format.

Figure 14. Generated LMM prompt (P_c (v2)).

Additional LMM prompt (P_c (v3))

Classify the image.
 Only care about precision/specificity: always output the most fine-grained label you can. Do not abstain. Do not output 'None'. If multiple fine-grained labels are plausible, choose the single most specific label you consider most likely.
 Output the thinking process in `<think>` `</think>` and the final answer in `<answer>` `</answer>` tags.
 The output answer format should be as follows: `<think>` ... `</think>` `<answer>`a single label or the word 'None' to abstain.`</answer>`.
 Please strictly follow the format.

Figure 15. Generated LMM prompt (P_c (v3)).

grained set in [10], that is: Flowers102 [36], Food101 [6] and OxfordPets [38]. Table 10 shows the performance of SpeciaRL on each test dataset, when trained on different domains. On each test set, the models' in-domain performance is in general the best among their out-of-domain results. Across the fine-grained test sets, the out-of-domain results remain consistent, generally falling within 8–10% of the in-domain performance. Interestingly, on the Flowers102 dataset, CUB provides a measurable positive transfer compared to the in-domain trained model (+1.1%). Despite variations among different training set, these results indicate that our proposed method achieves strong general performance even if trained on other distributions. Specifically, we use CUB as the training set in our main experiments as it is outside the evaluation sets of [10], to facilitate fair comparison against extensive baselines.

Impact of training set size. We evaluate the effect of training-set size on SpeciaRL by training models on subsets of increasing size sampled from the CUB training set. The

Fine-grained										
Test set	Training set	Prediction categorization						Metrics		
		S^+	S	S^-	G	A	W	spec. \uparrow	corr. \uparrow	HM \uparrow
Flowers102 [36]	Flowers102	0.0%	82.5%	2.7%	1.8%	0.0%	12.9%	<i>0.982</i>	<i>0.871</i>	<i>0.923</i>
	Food101	0.1%	66.5%	4.3%	10.4%	0.0%	18.7%	0.923	0.813	0.864
	OxfordPets	0.2%	72.8%	6.5%	4.7%	0.0%	15.8%	0.953	0.842	0.894
	CUB	13.6%	69.2%	5.0%	1.7%	0.0%	10.5%	0.976	0.895	0.934
Food101 [6]	Flowers102	1.5%	60.4%	6.4%	9.4%	0.0%	22.3%	0.919	0.777	0.842
	Food101	0.1%	79.7%	3.6%	7.5%	0.0%	9.2%	<i>0.949</i>	<i>0.908</i>	<i>0.928</i>
	OxfordPets	1.6%	60.2%	6.8%	9.1%	0.0%	22.2%	0.919	0.778	0.843
	CUB	1.2%	54.3%	5.8%	19.7%	0.0%	18.9%	0.860	0.811	0.835
OxfordPets [38]	Flowers102	4.3%	67.6%	8.5%	2.8%	0.0%	16.8%	0.958	0.832	0.890
	Food101	3.8%	44.1%	10.1%	33.7%	0.0%	8.3%	0.789	0.917	0.848
	OxfordPets	2.7%	87.2%	5.2%	0.0%	0.0%	4.9%	<i>0.986</i>	<i>0.951</i>	<i>0.969</i>
	CUB	2.1%	66.6%	4.5%	10.7%	0.0%	16.1%	0.923	0.839	0.879
CUB [51]	Flowers102	0.3%	49.2%	7.3%	14.3%	0.0%	29.0%	0.874	0.710	0.784
	Food101	0.0%	33.2%	9.0%	36.8%	0.0%	21.0%	0.739	0.790	0.763
	OxfordPets	0.2%	53.1%	3.8%	6.2%	0.0%	36.7%	0.936	0.633	0.755
	CUB	0.6%	92.7%	0.0%	0.0%	0.0%	6.7%	<i>1.000</i>	<i>0.933</i>	<i>0.965</i>

Table 10. Individual dataset results for SpeciaRL-7B trained with different fine-grained datasets. In-domain performance is highlighted in blue *italic* and best out-of-domain results on each test set is highlighted in **bold**. Note that CUB is an additional dataset, *i.e.* not part of the *fine-grained* test sets that are used in [10] and our main evaluation.

Sample size	Prediction categorization						Metrics		
	S^+	S	S^-	G	A	W	spec. \uparrow	corr. \uparrow	HM \uparrow
100	0.1%	53.1%	4.6%	8.7%	0.0%	33.5%	0.917	0.665	0.771
1000	0.2%	69.7%	5.4%	7.7%	0.0%	17.1%	0.938	0.829	0.880
2000	0.9%	91.6%	0.0%	0.0%	0.0%	7.5%	1.000	0.925	0.961
3000	0.6%	92.7%	0.0%	0.0%	0.0%	6.7%	1.000	0.933	0.965

Table 11. In-domain results of SpeciaRL-7B trained with different dataset sizes sampled from CUB, and evaluated with CUB test set.

number of epochs and all hyperparameters are kept identical to those used in the main paper. In-domain results in Tab. 11 show an increasing trend in both specificity and correctness as the dataset size grows, indicating the positive impact of additional training samples on SpeciaRL. For the main comparisons reported in the paper, we adopt the 3000 sample training subset from CUB as the default training dataset configuration.

For completeness, the out-of-domain results averaged over all *fine-grained* datasets are reported in Tab. 12. The model trained with less data show a small degradation in performance compared to the final model trained with 3000 samples. Performance in terms of HM stabilizes when the training set contains about 1000 samples. Yet, we observe that the correctness continuously increases with the increasing size of training set while the specificity exhibits a saturation about 2000 samples, followed by a decreasing tendency.

Training data diversity. To study how training-data composition affects performance, we compare SpeciaRL trained on a single source domain (3000 CUB samples) with a vari-

Sample size	Prediction categorization						Metrics		
	S^+	S	S^-	G	A	W	spec. \uparrow	corr. \uparrow	HM \uparrow
100	2.5%	64.9%	6.8%	7.6%	0.2%	18.0%	0.930	0.820	0.872
1000	3.2%	66.5%	6.2%	7.9%	0.0%	16.2%	0.933	0.838	0.883
2000	6.0%	64.8%	6.2%	6.4%	0.1%	16.6%	0.941	0.834	0.884
3000	5.6%	63.4%	5.1%	10.7%	0.0%	15.2%	0.920	0.848	0.883

Table 12. Out-of-domain results of SpeciaRL-7B trained with different dataset sizes sampled from CUB. Results are averaged over *fine-grained* datasets.

ant trained on an *in-domain* balanced mixture (500 samples from each of the six evaluation domains). This mixed training set includes CUB as well as all domains present in both the fine-grained and very fine-grained evaluation group. As reported in Tab. 13, the *in-domain* mixture-trained model expectedly outperforms the *out-of-distribution (OOD)* CUB-trained model, having observed those domains during training. Notably, the single-domain model still generalizes strongly to both fine-grained and very fine-grained unseen domains. We focus our analysis on this OOD setting to rigorously assess the generalization capability of SpeciaRL.

	CUB			Fine-grained			Very fine-grained		
	spec. \uparrow	corr. \uparrow	HM \uparrow	spec. \uparrow	corr. \uparrow	HM \uparrow	spec. \uparrow	corr. \uparrow	HM \uparrow
CUB	1.000	0.933	0.965	0.920	0.848	0.833	0.818	0.855	0.830
Mixed	0.995	0.889	0.939	0.963	0.878	0.918	0.863	0.860	0.852

Table 13. Comparison between SpeciaRL trained on a single domain (CUB) versus a mixture of samples from all available domains.

	Fine-grained		Very fine-grained	
	AR	κ	AR	κ
Qwen3-30B	0.90	0.84	0.92	0.82
Llama3-7B	0.75	0.64	0.69	0.48
$P_j (v_1)$	0.94	0.91	0.95	0.89
$P_j (v_2)$	0.91	0.87	0.91	0.80
$P_j (v_3)$	0.90	0.85	0.90	0.76

Table 14. LLM-as-a-judge validation across different models and prompt variants.

B.4.2. LLM-as-a-judge validation

Categorization agreement. We opt for large open-source LLMs to maximize their effectiveness as evaluators. Prior to model training, we (the authors) manually checked the LLM categorization of 100 samples per dataset to ensure human-aligned LLM judgment. For a more systematic analysis, we then compute the Agreement Rate (AR) and Cohen’s κ between Llama3-72B (ours) and alternative LLM verifiers (Qwen3-30B/Llama3-7B). Table 14 reports the results. Qwen3-30B shows *almost perfect agreement* with Llama3-72B ($\kappa > 0.81$), while Llama3-7B has *moderate agreement*, according to (Landis&Koch, 1997) [24]. Moreover, Llama3-72B is not sensitive to variations (v_i : Fig. 16, Fig. 17, Fig. 18) of the judge prompts P_j generated by ChatGPT, as evidenced by high AR and κ with our P_j (reported in Fig. 8).

Sensitivity to LLM-judge error. We conduct a controlled experiment on 1k training samples (CUB) by injecting label noise into the LLM-judge categorizations: with noise ratio ρ_e , we randomly upgrade/downgrade the predicted category (e.g., S^- to S or G). As shown in Tab. 15, SpeciaRL is largely insensitive to moderate noise levels, with only a minor degradation at $\rho_e = 10\%$. At $\rho_e = 25\%$, we observe a

ρ_e	Prediction categorization						Metrics		
	S^+	S	S^-	G	A	W	spec. \uparrow	corr. \uparrow	HM \uparrow
0%	3.2%	66.5%	6.2%	7.9%	0.0%	16.2%	0.933	0.838	0.883
5%	5.6%	65.3%	6.4%	5.4%	0.0%	17.3%	0.946	0.827	0.882
10%	3.3%	64.7%	6.6%	8.4%	0.0%	16.9%	0.928	0.831	0.877
25%	2.0%	64.5%	6.6%	10.5%	0.0%	16.4%	0.916	0.836	0.874

Table 15. Sensitivity of SpeciaRL to LLM-judge error. Results are averaged over *fine-grained* datasets.

noticeable drop in performance. Overall, SpeciaRL remains rather robust for $\rho_e \leq 10\%$, while higher noise levels start to degrade the training signal.

Additional LLM-as-a-judge prompt (P_j (v1))

Role: You are an expert AI verifier. You must classify a model's prediction against a ground_truth.

Task: You will receive exactly one JSON object. Output **only one category word** and nothing else.

Allowed Categories (output exactly one)

Specific, Less Specific, Generic, More Specific, Wrong, Abstain

Canonical Meanings

- **Specific:** exact match or direct synonym (including common name ↔ scientific name equivalence).
- **Less Specific:** correct but only a *closely related parent* of ground truth (nearby hypernym such as genus/family/model-variant parent).
- **Generic:** correct but *significantly broader* than ground truth (coarse hypernym).
- **More Specific:** prediction is *more specific* than ground truth (a subtype/instance under the ground truth).
- **Wrong:** incorrect, contradictory, malformed, unrelated, or contains multiple options/hedged alternatives.
- **Abstain:** refusal/uncertainty/none.

Deterministic Decision Procedure (apply in order)

1. If prediction is an abstention/refusal/uncertainty (e.g., "none", "cannot tell", "I don't know"): output **Abstain**.
2. If prediction is malformed, nonsense, unrelated, contradictory, or gives multiple options (e.g., "A or B", lists): output **Wrong**.
3. If prediction and ground_truth denote the same entity via exact match or direct synonym: output **Specific**.
4. If prediction is a *parent category* of ground_truth:
 - if the parent is close (e.g., genus for species): output **Less Specific**.
 - if the parent is broad/coarse (e.g., animal for dog): output **Generic**.
5. If prediction is a *child/subtype/instance* of ground_truth: output **More Specific**.
6. Otherwise: output **Wrong**.

Input Format:

```
{"ground_truth": "<the_ground_truth_label>","prediction": "<the_vlm_prediction>"}
```

Output Format: A single word from the allowed categories.

Prompt:

Apply the decision procedure to classify the following JSON object.
Output exactly one category word.

INPUT:

```
%s
```

Figure 16. Generated Prompt for the LLM-as-a-judge verifier.

Additional LLM-as-a-judge prompt (P_j(v2))

Role: You are an expert AI classifier (verifier). Your goal is to label the relationship between prediction and ground_truth.

Task: You will receive one JSON object. Output must be **only** one category word.

Categories

Specific, Less Specific, Generic, More Specific, Wrong, Abstain

Pre-processing Rules (apply before judging)

- **Normalize:** Treat case, punctuation, and surrounding whitespace as irrelevant.
- **Treat common name ↔ scientific name equivalence as a valid synonym match.**
- **If the prediction contains multiple candidates, alternatives, disjunctions (“or”, “/”, “;”) or a list of labels, classify as **Wrong**.**
- **If the prediction expresses refusal, uncertainty, or no-answer, classify as **Abstain**.**

Semantics

- **Specific:** Normalized exact match or direct synonym of ground truth.
- **Less Specific:** Correct but a *nearby hypernym* (close parent category).
- **Generic:** Correct but a *coarse hypernym* (much broader).
- **More Specific:** Correct but a *hyponym* (more specific than ground truth).
- **Wrong:** Anything else (incorrect, contradictory, malformed, unrelated, multi-answer).
- **Abstain:** Refusal or no-answer.

Input Format:

```
{"ground_truth": "<the_ground_truth_label>",  
 "prediction": "<the_vlm_prediction>"}
```

Output Format: One word: Specific | Less Specific | Generic | More Specific | Wrong | Abstain

Prompt:

Normalize then classify the following JSON. Output exactly one category word.

INPUT:

%s

Figure 17. Generated Prompt for the LLM-as-a-judge verifier.

Additional LLM-as-a-judge prompt (P_j(v3))

Role: You are an expert verifier for label correctness and specificity.

Task: Given one JSON object with `ground_truth` and `prediction`, output **only** the correct category word.

Output Categories

Specific, Less Specific, Generic, More Specific, Wrong, Abstain

Internal Decision Checklist (Do NOT output the checklist)

- **A) Abstention?**
If prediction is “none” / refusal / uncertainty → **Abstain**
- **B) Invalid / multi-answer?**
If prediction is malformed, gibberish, contradictory, unrelated, or includes multiple options/hedges → **Wrong**
- **C) Same meaning?**
Exact same entity or direct synonym (incl. common/scientific name) → **Specific**
- **D) Correct but different specificity?**
If prediction is a parent category of ground truth:
 - close parent → **Less Specific**
 - broad parent → **Generic**If prediction is a child/subtype/instance under ground truth → **More Specific**
- **E) Otherwise** → **Wrong**

Input Format:

```
{"ground_truth": "<the_ground_truth_label>","prediction": "<the_vlm_prediction>"}
```

Output Format: Return exactly one word from the category set and nothing else.

Prompt:

Classify the following JSON object. Return exactly one category word.

INPUT:

%s

Figure 18. Generated Prompt for the LLM-as-a-judge verifier.